Available online at www.sciencedirect.com

SCIENCE DIRECT®

Global and Planetary Change 44 (2004) 129–161

GLOBAL AND PLANETARY CHANGE

www.elsevier.com/locate/gloplacha

Analysis of extreme precipitation over Europe from different reanalyses: a comparative assessment

Olga Zolina[a,*], Alice Kapala[a], Clemens Simmer[a], Sergey K. Gulev[b]

[a]*Meteorologisches Institut, Universitaet Bonn, Auf dem Huegel, 20, D-53121, Germany*
[b]*P.P.Shirshov Institute of Oceanology, Moscow, Russia*

Received 11 November 2003; accepted 28 June 2004

Abstract

Statistical characteristics of daily precipitation in the reanalyses of the National Centers of Environmental Prediction (NCEP1 and NCEP2) and the European Center for Medium Range Weather Forecasts (ECMWF; ERA15 and ERA40) are intercompared with each other and with the in situ data assembled from different collections of station observations. Intercomparison is performed over the European continent. Precipitation statistics analyzed were the precipitation intensity, the parameters of Gamma distribution and the 99% percentiles of daily precipitation. NCEP1 and NCEP2 reanalyses show the higher occurrence of heavy precipitation than ECMWF products. Station data in comparison to the reanalyses show significantly higher estimates of heavy and extreme precipitation. Among the four reanalyses, NCEP2 demonstrates the closest to the station data estimates of extreme precipitation. The analysis of linear trends of statistical characteristics of heavy precipitation in ERA40 and NCEP1 for a 43-year period shows similarity of the trend patterns in winter and identifies strong local disagreements, resulting in the trends of opposite signs during summer. Interannual variability of statistical characteristics in different reanalyses is quite consistent over the Northern and Eastern Europe than in the mountain regions of the Southern Europe. Correlation between statistical characteristics of precipitation in different reanalyses and between the reanalyses and station data is 20–30% higher during the winter season.

Keywords: European precipitation; Statistical characteristics of daily precipitation; Linear trends; Reanalyses

1. Introduction

The short-term variability of European precipitation is crucially important due to the strong social and economic impacts of extreme precipitation anomalies, because extreme rainfalls give birth to floods on major

* Corresponding author. Tel.: +49 228 735181; fax: +49 228 735188.
E-mail address: olga.zolina@uni-bonn.de (O. Zolina).

0921-8181/$ - see front matter © 2004 Elsevier B.V. All rights reserved.
doi:10.1016/j.gloplacha.2004.06.009

European rivers. Experiments with coupled climate models report strong changes in the occurrence of heavy precipitation under warming conditions (Zwiers and Kharin, 1998). Hennessy et al. (1997) and Yonetani and Gordon (2001) found an increase of occurrence of extreme precipitation events in a warmer climate in coupled UKHI and CSIRO model experiments. Their results were confirmed by Watterson and Dix (2003), who analyzed five-member ensembles of climate experiments with the CSIRO Mark 2 model. Semenov and Bengtsson (2002) studied secular changes in the characteristics of extreme precipitation in greenhouse gas simulations with ECHAM4/OPYC3. They found that although the total number of wet days in Europe exhibits a pronounced decrease in the course of the transient climate experiment, the number of days with precipitation exceeding the 90% quantile has a tendency to grow as well as mean precipitation.

Precipitation variability over the European continent has been analyzed on the basis of station data and station-derived climatologies for both mean precipitation and the occurrence of heavy precipitation in many regional and continental scale studies. They describe regional changes of both secular and interannual nature, reporting about mostly increasing occurrence of extreme rainfalls (e.g. Dai et al., 1997; Frei and Schar, 2001). However, Klein Tank and Koennen (2003) noted spatial inhomogeneity of the trends patterns, which are largely influenced by the orography and subgrid-scale processes. In particular, Beniston et al. (1994) and Beniston (1997) showed a cyclic character of the winter snow precipitation in Alps, attributed to the occurrence of the high/low pressure episodes. Many authors associate these changes with variability in atmospheric circulation patterns, in particular with the North Atlantic Oscillation during the winter season (e.g. Hurrell, 1995; Hurrell and van Loon, 1997; Wanner et al., 2001; Corte-Real et al., 1998), pointing out that the NAO-associated projections in the mean and heavy precipitation represent a south–north dipole with the centers of action over the southern Europe and Scandinavia. This is supported by the analysis of the weather types (Plaut and Simonet, 2001; Plaut et al., 2001), implying increasing frequency of wet days and heavy precipitation in the Alpine region and southern Europe under dominating blocking regimes and the growing frequencies in the northern regions associated with zonal circulation regimes.

During the last decades, the National Centers of Environmental Prediction (NCEP) together with the National Center for Atmospheric Research (NCAR) and the European Center for Medium Range Weather Forecasts (ECMWF) produced dynamically consistent data sets for the needs of climate research, commonly known as reanalyses (Gibson et al., 1999; Kalnay et al., 1996; Kistler et al., 2001; Uppala et al., 2000; Kanamitsu et al., 2002). These products provide basic meteorological variables, including precipitation with high spatial and temporal resolution. In terms of continuity, these data can compete with the station data, by covering already several decades. However, the reanalyses data sets are primarily represented by the output of numerical weather prediction (NWP) system. Precipitation appears to be one of the most uncertain forecasted parameters in the reanalyses due to still poor skill of operational NWP models to account for all important physical mechanisms, which affect the atmospheric water cycle. Thus, these data must be extensively validated against alternative data sources and intercompared to each other before they are used for the analysis of precipitation variability on climate scale. An important question to address is the robustness of the description of precipitation extremes and changes in their occurrence in different reanalyses.

In this work, we approach this question for four major existing reanalyses (NCEP/NCAR, hereafter NCEP1, NCEP2, ERA15 and ERA40) over the European continent. We will quantify the extreme precipitation characteristics in every product and quantitatively assess the differences in the mean characteristics of precipitation extremes and their variability patterns. This will allow us to identify common characteristics and their spatial distribution in different data sets, which can be used for further validation of the reanalyses against observational data. In Section 2, we will briefly describe the four reanalyses used in this study as well as station data employed for the comparisons. Section 3 describes the methods of quantification of heavy precipitation. Short comparison of the mean precipitation characteristics, standing in this study as a background comparative assessment, is given in Section 4. Section 5 is concentrated on the comparison of mean statistical

characteristics of heavy precipitation from different reanalyses over Europe and their interannual variability. Section 6 shows some comparisons of the precipitation statistics with the station data. In conclusive Section 7, we summarize the results and discuss them in the context of potential applications of reanalyses for studies of European precipitation extremes.

2. Data and preprocessing

The four reanalysis products have been generated in the off-line runs of the state-of-the-art operational atmospheric general circulation models (AGCM), including their data assimilation systems. These data assimilation systems were frozen during the production period, while data input to the system may have changed over the years (e.g. White, 2000). Precipitation in reanalyses is generated by two mechanisms: convective precipitation, falling from the convective clouds, and large-scale (stratiform) precipitation, associated with the frontal or dynamical systems. Both components are realized through the convective schemes used in NWP models. ECMWF ERA15 Reanalysis (Gibson et al., 1999) covers the period 1979–1993 and is based on the operational T106 AGCM. The model uses the mass flux convection scheme by Tiedtke (1989). The ECMWF ERA40 (1958–2001) system formulation (Uppala et al., 2000; Kallberg, 2002) used a T159 resolution AGCM and assimilated SSM/I radiances as well as ERS-1 and ERS-2 data. Although the computation of horizontal derivatives in ERA15 and ERA40 was based on the spectral numerical representation (T106 and T159, respectively), all physical parameterizations, including those of precipitation, were run on the reduced N80 Gaussian grid with a resolution in longitudinal direction, varying over European region from 1.25° to 3° (Gibson et al., 1999). Thus, the impact of resolution on precipitation fields in ERA products is significantly reduced. Many validation studies (e.g. Arpe et al., 2000; Kallberg, 2002) reported about the strong impact of the spin-up on precipitation in short-range forecasts of ERA15, especially over tropics and mid-latitudinal storm tracks. Stendel and Arpe (1997) and Arpe et al. (2000) showed that the use of 24- or 12-hourly forecasts instead of 6-hourly ones tends to partly correct the spin-up bias in precipitation fields. In ERA40 reanalysis, the spin-up effect on the convective precipitation was considerably reduced in comparison to ERA15 (Kallberg, 2002); however, its impact still remains in the estimates of the global water cycle (Hagemann et al., 2002).

NCEP1, covering the period from 1948 onwards (Kalnay et al., 1996; Kistler et al., 2001), is based on the T62 operational NCEP model in which the physical parameterizations were run on 192×94 Gaussian grid (1.92×1.875°). The model dynamics and physics follows Kanamitsu et al. (1991) with, however, implementation of a simplified Arakawa-Schubert convective parameterization scheme (Pan and Wu, 1994), which shows a better prediction of precipitation and more realistic precipitation climatology. Assimilation included, besides radiosondes, the dropsondes and pibals, marine and continental winds from different sources. NCEP2 reanalysis (Kanamitsu et al., 2000, 2002) was run at the same resolution (T62) as NCEP1, covering the period from 1979 onwards. This product is free from many known biases and errors, which have been identified in the NCEP1. In particular, an incorrect parameterization of horizontal moisture diffusion has been corrected along with an unrealistically high oceanic albedo. An important improvement was the updated precipitation parameterizations and more realistic cloud-top cooling. A simple assimilation scheme of rainfall has been employed for updating soil moisture. Details of the system formulations for the different reanalyses can be found in Gibson et al. (1999), Kalnay et al. (1996), Kanamitsu et al. (2000, 2002) and Uppala et al. (2000). Comparative assessments can be also found in Stendel and Arpe (1997), Arpe et al. (2000) and Kanamitsu et al. (2002). In particular, Arpe et al. (2000) pointed out considerable overestimation of precipitation over continents in the NCEP reanalyses in the Northern Hemisphere summer.

For the intercomparison, we used the output from all reanalyses with 6-hourly temporal resolution, from which we derived daily precipitation. Available spatial resolution of the output was 1.92×1.875° for NCEP1 and NCEP2 and somewhat higher in ERA reanalysis. The different spatial resolutions among the data sets were interpolated onto 2×2° spatial resolution by the modified method of local procedures (Akima, 1970). Although this procedure itself does not result in Gibbs

oscillations, we understand that for this continental-scale study ERA15 and ERA40 reanalyses were downgraded (in comparison to the original resolution) for the comparison with NCEP products. Total precipitation values (when unavailable) were derived from the convective and stratiform components. For a pilot intercomparison with station data, we used daily precipitation from the Royal Netherlands Meteorological Institute (KNMI) collection, known as European Climate Assessment (ECA) daily data set (Klein Tank et al., 2002), which has been merged with the regional German Weather Service (DWD) collection. The merged data set consists of about 306 stations, 140 of which provide measurements for periods from 50 to 100 years and 45 for more than 100 years starting from the mid-19th century onwards. The data set has a quite inhomogeneous spatial coverage with the highest station density in Central Europe and a considerable drop of the number of observational sites in Southeastern and Eastern Europe. The precision of most of rain gauges is 0.1 mm, and thus, daily precipitation from the rain gauge observations is reported with the accuracy of 0.1 mm. In order to provide comparability, we set all daily precipitation sums smaller than 0.1 mm to zeros in the reanalyses time series. These small values occur quite frequently, because for instance in many European areas in ERA15 and NCEP1 it rains (if only in a small amount) practically every day. This resulted in the drop in the number of wet days by 5% to 30% (no figure shown). The largest differences are observed in NCEP1 and ERA15 in the Central and Eastern Europe. This ad hoc correction changing estimates of the wet days and precipitation intensity has a smaller impact on the mean precipitation values (from 1% to 3% for most locations).

3. Strategy and methods

In order to quantify the characteristics of extreme precipitation, we use the parameters of the Gamma distribution of daily precipitation. The effectiveness of this distribution for the analysis of daily precipitation was demonstrated for both model and observational data by Groismann et al. (1999), Katz (1999), Semenov and Bengtsson (2002), Watterson and Dix (2003), and others. The Gamma distribution is a positively skewed distribution bounded by zero on the left. The Gamma-distribution probability density function (PDF) for daily precipitation values $F(x)$ is then given by:

$$F(x) = \frac{\left(\frac{x}{\beta}\right)^{\alpha-1} e^{-\frac{x}{\beta}}}{\beta\Gamma(\alpha)}, \alpha>0,\ \beta>0 \qquad (1)$$

where $\Gamma(\alpha)$ is the Gamma function, α is the shape parameter and β is the scale parameter of the distribution. These two parameters determine the Gamma-distribution PDF. The shape parameter α is non-dimensional and determines the skewness of the Gamma PDF, shifting it to the left with small α values and to the right with high α values. The scale parameter β, which has the dimension of variable analyzed, steers stretch and squeeze of the PDF. The effectiveness of the Gamma distribution for the analysis of precipitation data is justified by the possibility to account for both variations in mean and variance through the shape and scale parameters. Although it is clear in general that the growing shape parameter results in higher probability of extreme values, as well as that the increase of scale factor implies higher occurrence of extremes, the joint effect of the two parameters on the occurrence of extremes is quite complicated. In Fig. 1, we illustrate the connection between the parameters of Gamma distribution for the extreme values. We show the values of daily precipitation, corresponding to the 99% percentile of the cumulative distribution function (CDF) in coordinates of the shape and scale parameters, overplotted with the values of mean precipitation ($\alpha\beta$) in the background. The higher percentile of Gamma CDF is considered; the smaller curvature of the fixed daily precipitation, corresponding to these percentiles, is observed. For a fixed mean precipitation, the growing scale parameter implies increasing of the percentile for a relatively large (more than 10 mm/day) precipitation value. Quantitative estimation of the shape and scale parameters was performed using maximum likelihood method of Greenwood and Durand (1960), based on $\ln(\langle x\rangle)-\langle\ln(x)\rangle$, $\langle\rangle$ being the averaging operator, which is more effective than the traditional moment estimators (Wilks, 1990, 1995) and more accurate for the data used than the Thom (1958) method. From the Gamma distribution, we have derived the other statistical characteristics of

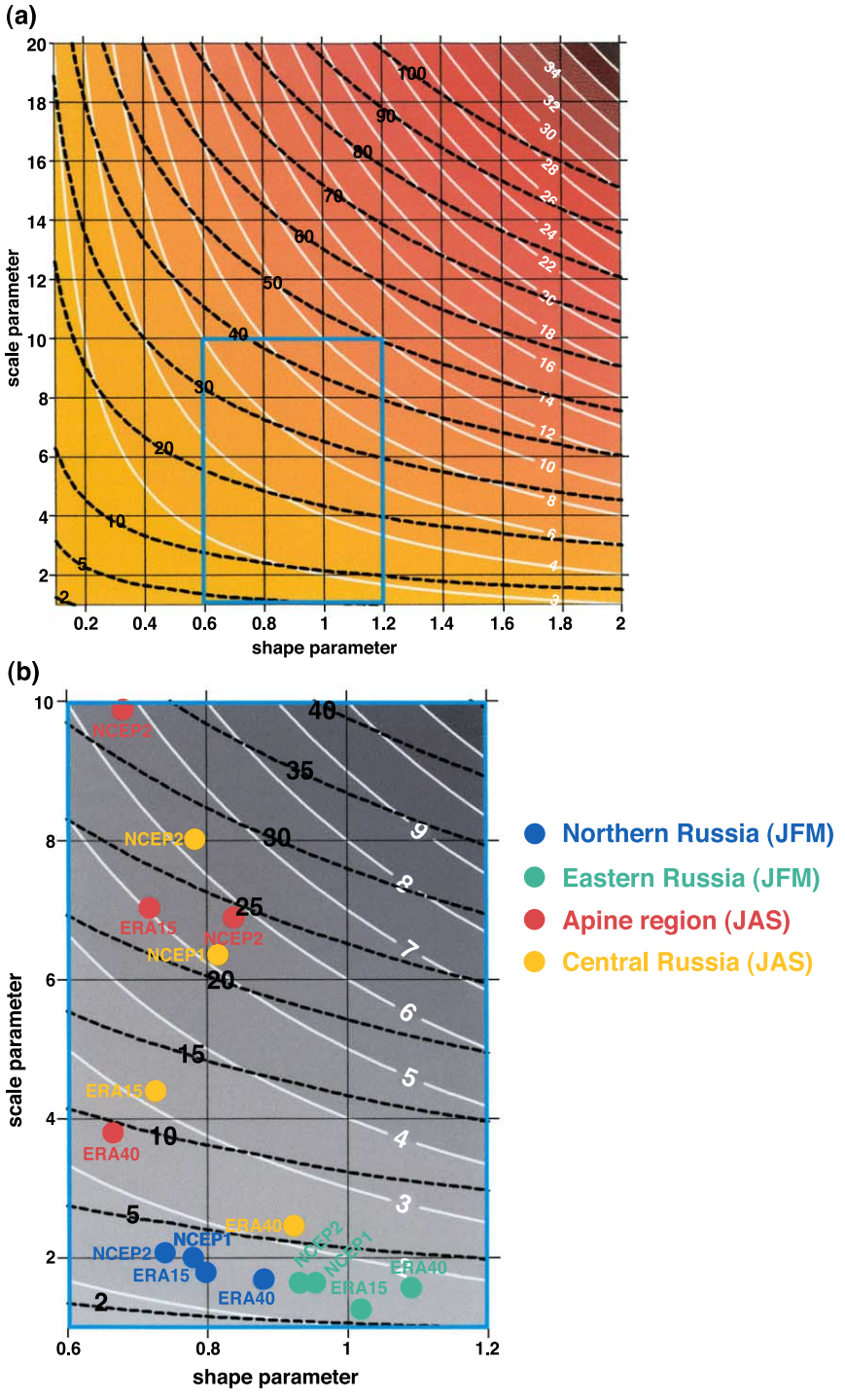

Fig. 1. Diagram showing mean precipitation intensity (white contours) and precipitation values corresponding to 99% percentile (dash black contours) in the coordinates of shape and scale parameters (a) and comparisons of reanalyses in the locations in the Northern Russia (47E,63N, blue), Eastern Russia (51E,49N, green), Alpine region (11E,45N, red) and in Central Russia (35E,53N yellow) (b). (For interpretation of the references to colour in this figure legend, the reader is referred to the web version of this article.)

daily precipitation, such as different percentiles and others.

We analyzed in this paper the seasonal statistics of daily precipitation, derived for winter (JFM), spring (AMJ), summer (JAS) and autumn (OND). Climatological statistics can be of course estimated for individual months. However, since we were looking on interannual variability, we had to meet the proper sampling requirements for the estimation of statistical parameters. Even for seasonal resolution, some dry areas in Northern Africa show a very few wet days per season especially after the elimination of days with very small precipitation values. We estimated the accuracy of the approximation of empirical CDFs by Gamma distribution, using a Kolmogorov-Smirnov (*k-s*) test with the null-hypothesis, that the empirical data of daily precipitation are drawn from the Gamma distribution. This test was performed for the grid points with more than 5 days with precipitation per season according to the criterion of Semenov and Bengtsson (2002). Table 1 shows the number of grid points for which this hypothesis was rejected at 90% significance level. Most of these rejected locations were identified in the Northern Africa and south-eastern Europe. Reanalyses of ECMWF show in general somewhat larger number of rejected locations than NCEP reanalyses. Normally, the number of rejected grid cells in summer is slightly higher than in winter. Although the analysis of station data gives comparable estimates with NWP products, they are hardly comparable on continental scale due to very inhomogeneous coverage of station data. Semenov and Bengtsson (2002) performed similar analysis of the results of scenario run of ECHAM4 and reported 3% to 5% of the rejected grid cells for all continents, that is somewhat lower than our estimates for most reanalyses. Locations with either smaller than five wet days per season or where the goodness of fit of Gamma distribution was not supported by *k-s* test at 90% significance level were eliminated from the analysis.

Table 1
The percentage of grid points for which the goodness of fit of the Gamma distribution falls at 90% significance level for different seasons and different data sets

Data set	JFM	JAS
ERA15	16.6	18.3
ERA40	2.6	11.4
NCEP1	8.2	8.9
NCEP2	6.5	9.3
Stations	9.6	7.5

Our strategy was to compute statistical characteristics (e.g. the parameters of Gamma distribution) and to analyze their climatological values and variability in the four reanalyses for the common period of overlap (1979–1993). Some comparisons were, nevertheless, performed for a longer period (1958–2001) for NCEP1 and ERA40 reanalyses. Analysis of interannual variability was based on the estimation of linear trends in the statistical parameters and the leading empirical orthogonal functions (EOFs) for the shape parameter, scale parameter and percentiles of the Gamma distribution.

4. Comparison of precipitation climatologies from different reanalyses

We start with a brief comparative overview of climatological precipitation characteristics over the European continent. More detailed comparisons of reanalyses over the European continent as well as validation of the mean precipitation can be found in Stendel and Arpe (1997), Arpe et al. (2000), Kanamitsu et al. (2000, 2002), Gibson et al. (1999) and others. Fig. 2a–d shows the spatial distribution of mean precipitation for winter (JFM) and summer (JAS) computed from ERA40 and NCEP2 reanalyses for the period from 1979 to 1993. Both data sets exhibit a clear climatological pattern with maximum precipitation in the coastal regions of the West Europe in winter, and in Central and Eastern Europe in summer. During the winter season, ERA40 (Fig. 2a) shows 10–15% higher precipitation than NCEP2 (Fig. 2b) nearly everywhere, while in summer NCEP2 precipitation is much higher (Fig. 2c,d). The largest differences of 2–3 mm/day occur over Scadinavia, Eastern and Southern Europe. These tendencies are similar for the comparison of NCEP1 and ERA15 for the same period (no figure shown), i.e. NCEP1 and ERA15 are closer to their heirs than to the foreign data sets.

Fig. 2e–h shows the differences between NCEP2 and NCEP1 (Fig. 2f,h) as well as between ERA40 and ERA15 (Fig. 2e,g) for mean precipitation in winter

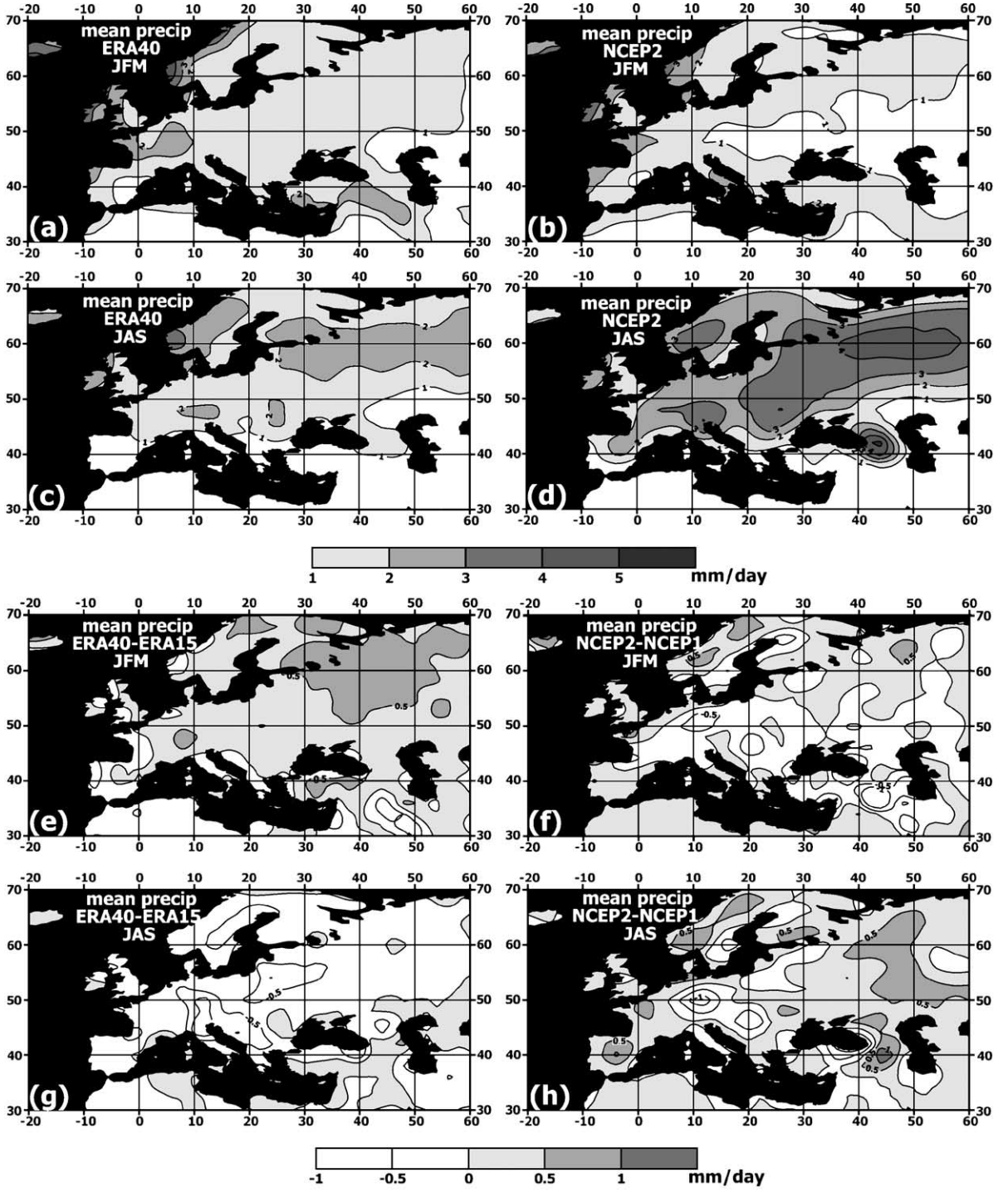

Fig. 2. Climatological precipitation (mm/day) over Europe for winter (a, b) and summer (c, d), derived from ERA40 (a, c) and NCEP2 (b, d) reanalyses for the period from 1979 to 1993, and differences in mean precipitation (mm/day) "ERA40–ERA15" (e, g) and "NCEP2–NCEP1" (f, h) for winter (e, f) and summer (g, h) for 1979–1993.

and summer (1979–1993), indicating how the development of operational systems affected the precipitation climatologies. The upgrade of the ECMWF operational system resulted in an increase of the mean winter precipitation (up to 0.5 mm/day in Swiss Alps and Northeast Europe) and a decrease of the mean summer precipitation almost everywhere with the largest differences up to 1–1.5 mm/day in Central and Eastern Europe. Comparison of the two NCEP reanalyses does not show such a regular pattern. This can be partly explained by the largely reduced spectral noise in precipitation fields in NCEP2 (Kanamitsu et al., 2002). Nevertheless, in both winter and summer NCEP2 shows substantial higher values compared to NCEP1 over Scandinavia and in the Eastern Europe, where differences amount to 0.5–1 mm/day. During summer locally high positive differences are also found over Iberian Peninsula and Caucasus. Kanamitsu et al. (2002) compared winter (DJF) precipitation rates from NCEP2 and NCEP1 and also found

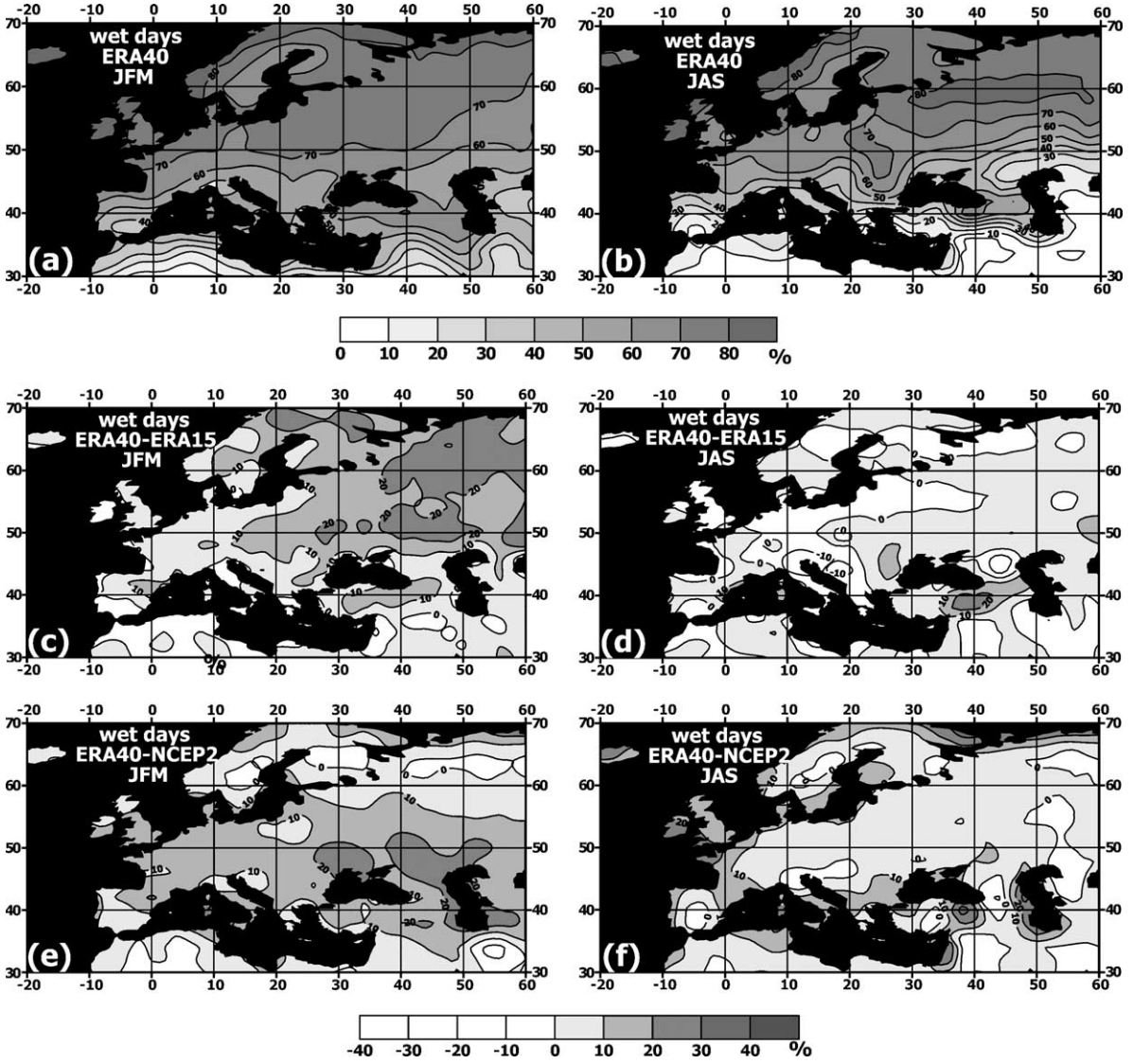

Fig. 3. Wet days probability (%) in ERA40 reanalysis for winter (a) and summer (b), as well as winter (c, e) and summer (d, f) differences in the wet days probability between ERA40 and ERA15 (c, d) and between ERA40 and NCEP2 (e, f).

besides less noisy fields in NCEP2, higher values over Scandinavia.

Statistical parameters of Gamma distribution of daily precipitation are based on the wet days, which were defined in this study according to the criterion 0.1 mm/day (Section 2). In Fig. 3a,b, we show as reference the number of wet days (expressed in percent of the total number of days during the season) for winter and summer in ERA40 reanalysis. The highest number of wet days (more than 80%) is observed in the northern Europe in winter and in the Eastern Europe in summer, decreasing in the southern Europe to the values of 10–20%. In winter, ERA40 in comparison to ERA15 shows significant increase of

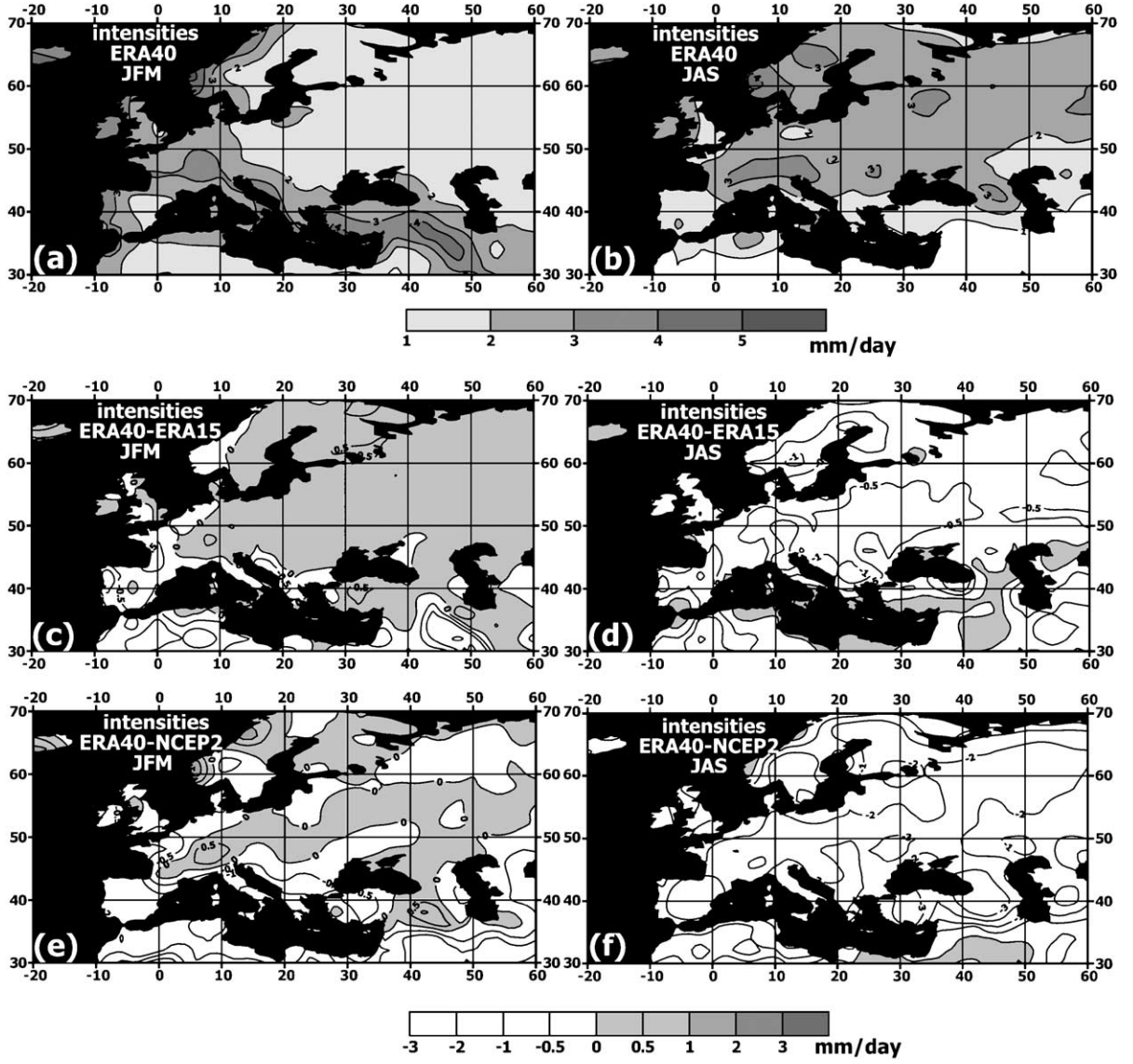

Fig. 4. Mean precipitation intensities (mm/day) in ERA40 reanalysis for winter (a) and summer (b), and differences in the mean precipitation intensity (mm/day) between ERA40 and ERA15 in winter (c) and summer (d), as well as between ERA40 and NCEP2 in winter (e) and summer (f).

the number of wet days from less than 10% in the southeastern Europe to more than 20% in the Central Eastern and Northern Europe (Fig. 3c). During summer, the number of wet days in ERA40 is slightly higher than in ERA15 in the southeastern Europe and lower in the Central Europe (Fig. 3d). Fig. 3e,f shows that in most locations ERA40 diagnoses a higher number of wet days than NCEP2. The highest differences of 20–30% are observed in the southern Russia in winter and over the coastal western Europe in summer. Comparison of the number of wet days between NCEP1 and NCEP2 (not shown) does not show a regular pattern in differences. Roughly one can say about slightly higher number of wet days in NCEP2 in the Central and eastern Europe in both winter and summer and mostly higher number of wet days in NCEP1 in winter over Scandinavia and northern Europe.

Differences in the number of wet days in different reanalyses (Fig. 3) imply that the conclusions drawn from the comparisons of mean precipitation may not necessarily hold for the precipitation intensities (daily precipitation values averaged over wet days). Fig. 4 shows the comparison for precipitation intensities between ERA40 and ERA15 reanalyses and between ERA40 and NCEP2 reanalyses. Considerably higher number of wet days in ERA40 in comparison to ERA15 in winter (Fig. 3c) results in substantially smaller differences in precipitation intensities between these two reanalyses (Fig. 4c) than those obtained for the mean precipitation values in the Northern Russia (Fig. 2e). In summer (Fig. 4d), differences in the number of wet days between ERA40 and ERA15 result in more continuous (in comparison to the differences in mean precipitation) pattern, indicating stronger precipitation intensities in ERA 15 than in ERA40. Fig. 2a,b shows a systematically slightly higher mean winter precipitation in ERA40 in comparison to NCEP2. The larger number of wet days in ERA40 in winter results in the pattern (Fig. 4c), showing smaller precipitation intensities in ERA40 over most of regions of the Western continental and Southern Europe. In summer, NCEP2 shows higher precipitation intensities than ERA40 (Fig. 4e) that agrees with the pattern of differences in mean precipitation. However, the relative differences are stronger for intensities than those for the mean precipitation due to a larger number of wet days in ERA40.

5. Statistical characteristics of heavy and extreme precipitation in different NWP products

5.1. Mean parameters of heavy precipitation

We turn now to the analysis of parameters of the Gamma distribution for winter (JFM) and summer (JAS) seasons in the different reanalyses. Fig. 5a–d shows the spatial distribution of the mean shape parameter for both seasons derived from ERA40 (Fig. 5a,c) and NCEP2 (Fig. 5b,d) for the period 1979–1993. Fig. 5e–h shows "ERA40–ERA15" (Fig. 5e,g) and "NCEP2–NCEP1" (Fig. 5f,h) seasonal differences in the shape parameter. For most areas in all four reanalyses, the shape parameter is smaller than 1. Higher than 1 values, implying an over-exponential form of the precipitation distribution, are observed in the northeastern Europe, where shape parameter may amount to 1.2 in ERA40 during winter.

During winter in all products, the shape parameter grows from the minimum values in the southern Europe to its maxima in the northeastern Europe, implying the growing probability of extreme precipitation in the Northern European regions. In summer, maximum values of the shape parameter are observed in the Central and Eastern European regions in all reanalyses. Despite a general qualitative similarity of spatial patterns of the shape, quantitative differences between different products are strong. NCEP1 shows a much stronger spatial inhomogeneity of the shape parameter in Central European regions compared to NCEP2. We can hypothesize that the higher spatial inhomogeneity in NCEP1 may be associated with a smoother topography used in NCEP2 (Kanamitsu et al., 2000, 2002). In this respect, it is interesting to note that the assimilation of Xie and Arkin (1997) 5-day mean rainfall for the adjustment of soil moisture and the implementation of convective parameterizations in the NCEP2 (Kanamitsu et al., 2000) did not result in increasing spatial inhomogeneity of the skewness. In winter, NCEP2 shows slightly higher than NCEP1 shape parameter in the Eastern Europe and over Norway and slightly lower shape parameter over the western Europe (Fig. 5f). Fig. 5h shows that during summer the shape parameter in NCEP1 is higher than in NCEP2 with the largest differences in the Central and Eastern Europe (up to 30% of mean values). Fig. 3e,g compares winter and summer shape parameter in

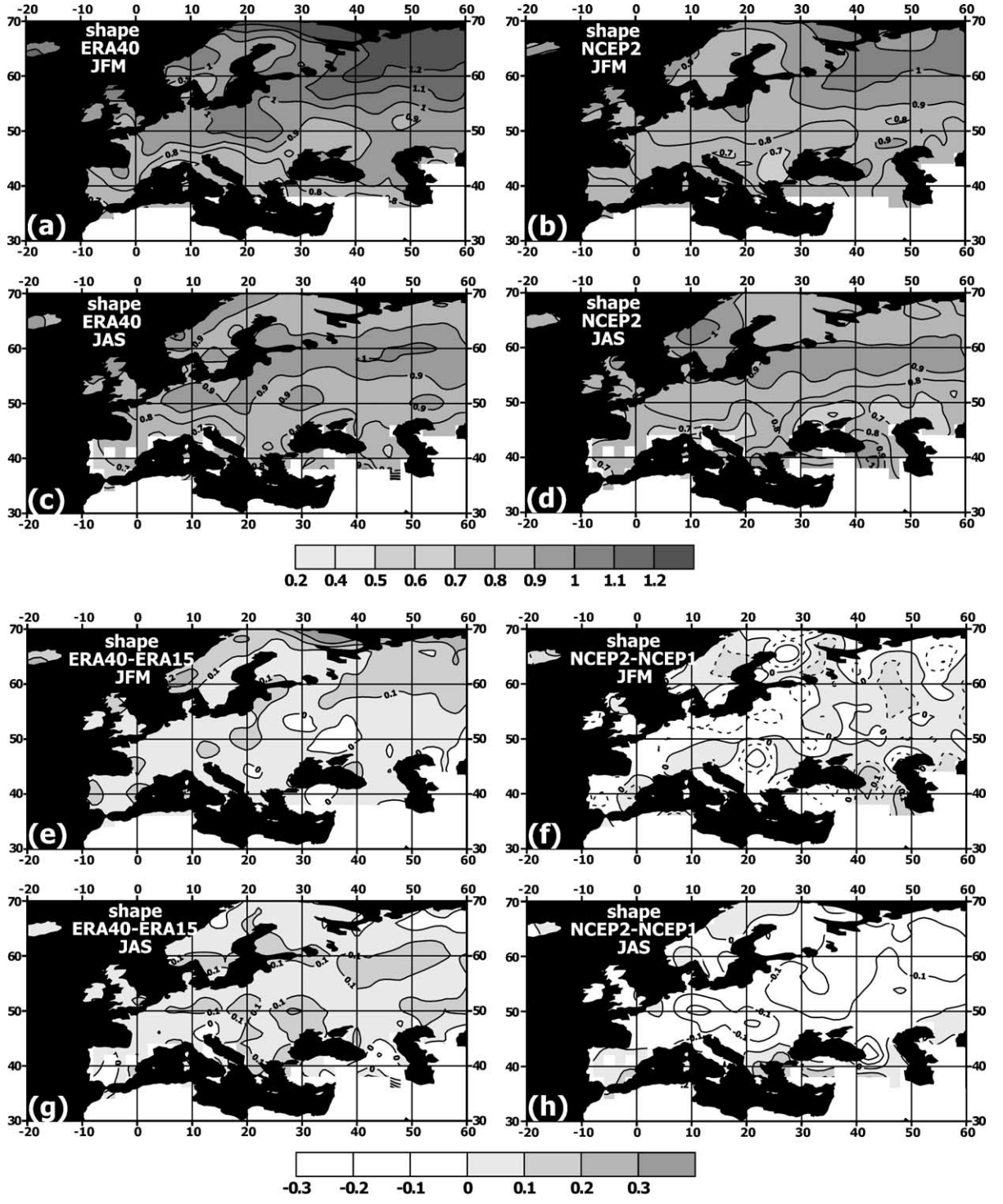

Fig. 5. Climatological mean shape parameter for winter (a, b) and summer (c, d) seasons, derived from ERA40 (a, c) and NCEP2 (b, d), as well as differences in shape parameter "ERA40–ERA15" (e, g) and "NCEP2–NCEP1" (f, h) for winter (e, f) and summer (g, h) seasons for the period 1979–1993.

ERA40 and ERA15. During winter, the largest increase of the shape parameter by 0.1–0.2 is observed in the northern European regions. During summer, this increase ranges within 0.15 with the local maximum in the Eastern Europe. Growing shape parameter implies the higher probability of extreme and heavy precipitation in ERA40 with respect to ERA15. Among all four reanalyses, ERA40 shows on average the highest shape parameter (largest probability of heavy rainfall) and ERA15 demonstrates the smallest shape factor, implying the smallest occurrence of precipitation extremes.

Comparisons of the scale parameter (Fig. 6a–d) show that in general it closely follows the pattern of the precipitation intensity, implying pattern correlation of 0.83–0.95 with a maximum for ERA40 in summer and minimum for NCEP products in winter. This was also noted by Semenov and Bengtsson (2002), who reported pattern correlation of more than 0.9 between the scale parameter and precipitation intensity. The highest values (associated with higher occurrence of heavy and extreme rainfall) observed for NCEP precipitation agree well with the higher mean precipitation intensities in NCEP products in comparison to those of ECMWF, especially in summer (Fig. 4). The mean values of the scale parameter vary from 1–3 mm/day in the Central and Eastern European region in winter to 8–10 mm/day in the areas of high precipitation over Iberian Peninsula and in the mountain regions (Caucasus, Alps) in summer. Among the four reanalyses, the highest scale parameter is observed in NCEP2 for both winter and summer and the smallest values of scale parameter are diagnosed by ERA40. Note that the development of the NCEP operational system (NCEP1 to NCEP2) resulted in a general increase of the scale parameter (Fig. 6f,h), while ERA40 shows the decrease of the summer scale factor everywhere and the winter values in the Western Europe with respect to ERA15 (Fig. 6e,g).

The occurrence of extreme precipitation depends on both scale and shape parameter. In order to assess the differences in the extreme precipitation diagnosed by the different products, we estimated the precipitation values corresponding to 99% percentile of Gamma CDF. In Fig. 7, we show spatial distribution of the precipitation corresponding to 99% percentile in ERA40 and NCEP2 for winter (Fig. 7a,b) and summer (Fig. 7c,d). In general, they follow to the spatial distribution of mean precipitation, but exhibit a much larger range, varying from 5 to 25 mm/day in winter and growing up to 40 mm/day in NCEP2 in summer. NCEP gives slightly higher values than ERA in the winter season and much higher values during summer in accordance with generally higher mean precipitation in NCEP products (Fig. 2). Fig. 7e–h shows "ERA40–ERA15" and "NCEP2–NCEP1" differences in precipitation values corresponding to 99% percentile for winter (Fig. 7e,f) and summer (Fig. 7g,h). In winter, ERA15 shows smaller 99% values than ERA40 over most of the eastern and southern European regions. At the same time, in Northwestern Europe the 99% percentile precipitation values are smaller in ERA40. In summer, precipitation values for 99% percentile in ERA15 are almost everywhere higher in comparison to ERA40 with the largest differences observed over Scandinavia and in the Southern Europe. NCEP2 shows primarily higher than NCEP1 precipitation values for 99% percentile during both winter and summer with the highest difference of 10–15 mm/day during summer in the Southern Europe. Comparisons of precipitation values corresponding to 99% percentile (Fig. 7) show that they are primarily driven by differences in the scale parameter of Gamma distribution (Fig. 4), especially in summer and in mountain regions. At the same time, in the Northern and Central Russia in winter, shape parameter may considerably contribute to the differences between different products. In Fig. 1b, we show comparisons for several locations on the α,β-diagram, overplotted with mean precipitation intensity and 99% percentile. Winter differences between different products over the Northern and Eastern Russia primarily imply a scatter along the shape parameter axis. On the other hand, summer ensembles over Alpine region and in Central Russia are mostly scattered along the β-axis. Summer differences between different products in the Northern Russia represent a combined effect of the shape and scale parameters on extreme precipitation.

5.2. Interannual variability of statistical characteristics of European precipitation

We characterized secular changes in statistical characteristics of daily precipitation over Europe by

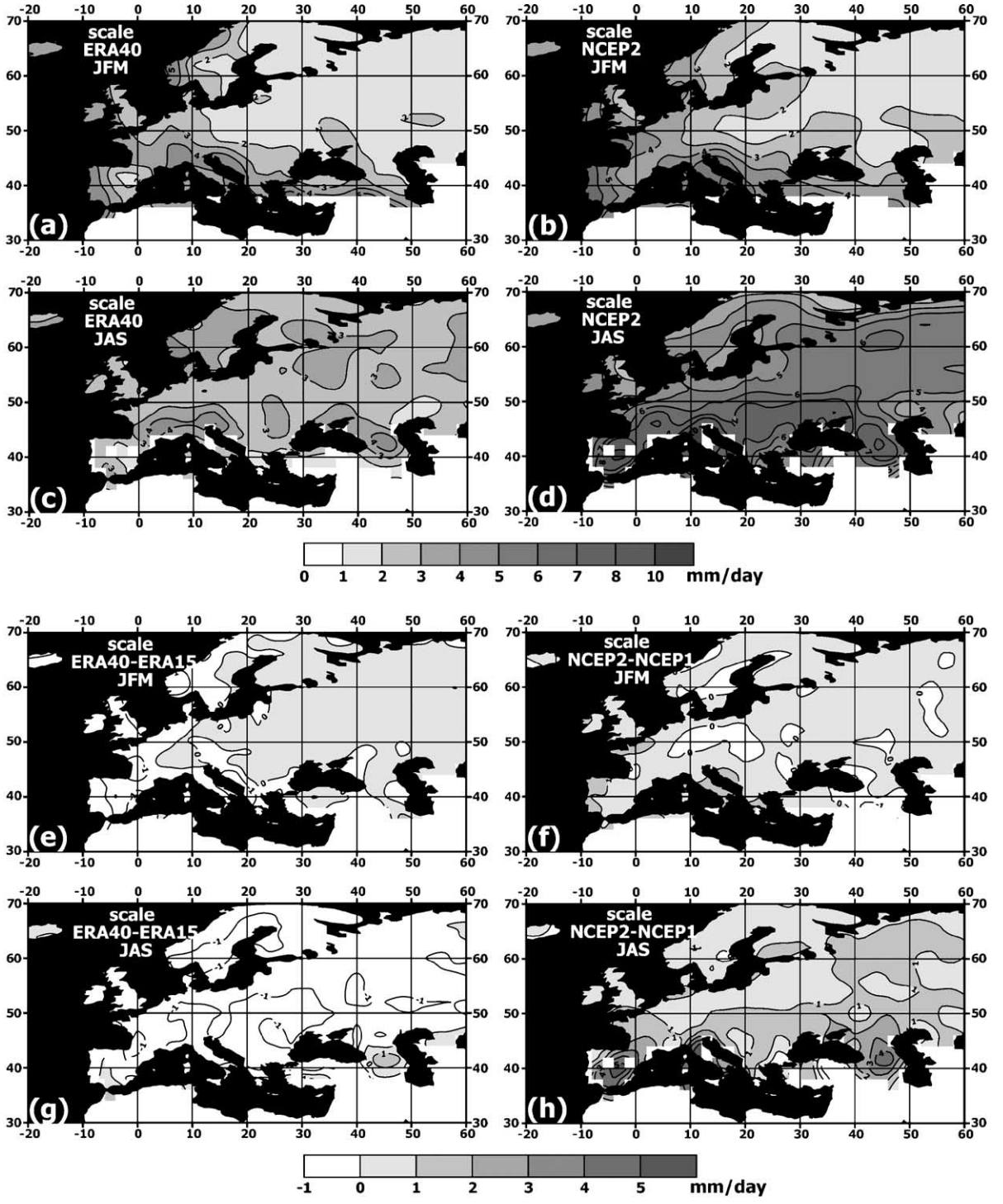

Fig. 6. Climatological mean scale parameter (mm/day) for winter (a, b) and summer (c, d) seasons, derived from ERA40 (a, c) and NCEP2 (b, d), as well as differences in scale parameter (mm/day) "ERA40–ERA15" (e, g) and "NCEP2–NCEP1" (f, h) for winter (e, f) and summer (g, h) for 1979–1993.

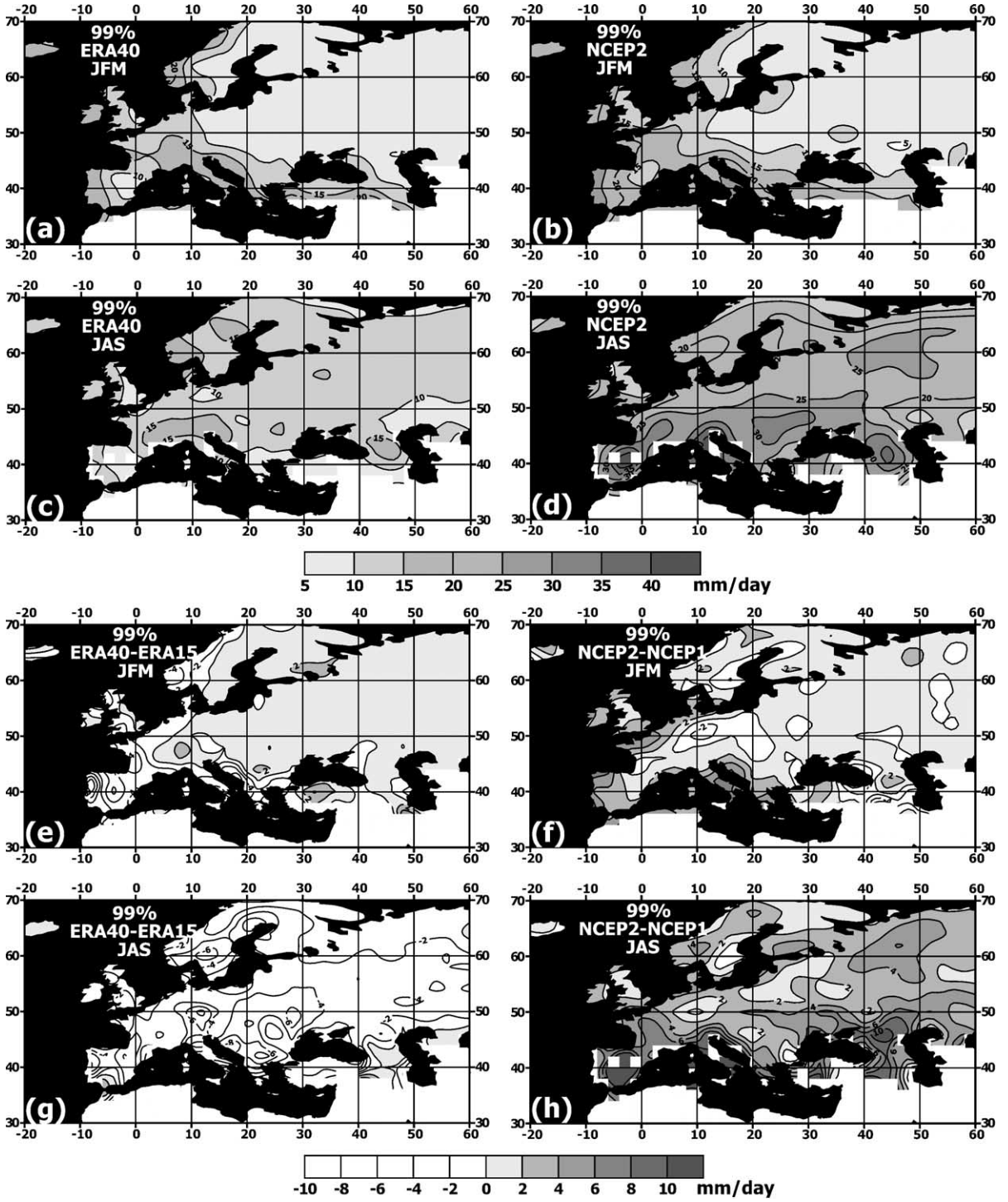

Fig. 7. Precipitation values corresponding to 99% percentile (mm/day) in ERA40 (a, c) and NCEP2 (b, d) for winter (a, b) and summer (c, d) as well as differences in 99% precipitation "ERA40–ERA15" (e, g) and "NCEP2–NCEP1" (f, h) for winter (e, f) and summer (g, h).

the linear trends of the shape and scale parameters. Linear trends were computed for the common 43-year period (1958–2000) of ERA40 and NCEP1. Fig. 8 shows estimates of linear trends for both seasons along with their statistical significance according to the Student's t-test. This test has been additionally controlled by the Hayashi (1982) reliability ratio, which considers the confidence intervals and introduces the quantitative measure of the statistical significance of trends and for short time series may show quite wide intervals, even if the t-test is formally satisfied for a given percentage. In winter (Fig. 8a,b), both products show significantly positive trends in the shape parameter over Western Scandinavia and Central and Southern Russia and significantly negative trends in Southwestern Europe (with however, stronger magnitude for NCEP1) for α. Trends of the opposite sign are locally observed in the Northeastern European Russia. We note that trend estimates in shape parameter are quite sensitive to the ad hoc elimination of small precipitation values (smaller than 0.1) from reanalyses. If we compute trends for the original time series with these small values (no figure shown), there will be drastic differences between ERA40 and NCEP1 reanalyses over the Central and Eastern European regions, where ERA40 would show significantly positive trends, while NCEP1 would diagnose negative tendencies over the last four decades. Summer differences in the linear trend patterns (Fig. 8c,d) are very pronounced in the Central and Southern Europe. ERA40 diagnoses continuous pattern of positive trends, while NCEP1 shows negative trends, implying a decrease of the probability of extreme precipitation in this product. Winter trend patterns in the scale parameter (Fig. 8e–h) are quite consistent in both reanalyses, showing a north–south dipole trend pattern with the positive trends over the Northern Europe and primarily negative trends in the Central and Southern Europe. Note that both positive and negative trends are somewhat stronger in NCEP1. However, in summer strong differences in the trend estimates are observed over the Southern Europe, where ERA40 shows strong negative trends and NCEP1 diagnoses increasing β (Fig. 8g,h). Disagreement is also observed over Scandinavia, where trends are weakly positive in ERA40 and strongly negative in NCEP1. Large differences occur over the Alpine region (strongly negative trends in ERA and significant positive trends in NCEP). Summer trend patterns are reasonably more noisy than winter ones, being largely affected by mesoscale convective precipitation components. The observed differences in the estimates of linear trends can be caused by many reasons. Since the largest differences are observed in summer season, they should be attributed to the representation of the convective precipitation in different reanalyses. Some disagreements can be partly explained by differences in the data assimilation input in the ECMWF and NCEP systems. Hypothetically, assimilation of Vertical Temperature Profile Radiometer (VTPR) and Television Infrared Operational Satellite (TIROS) Operational Vertical Sounder (TOVS) starting from 1972 and ERS winds (from 1991) could lead to secular tendencies in ERA40 in comparison to NCEP1, although one should expect first of all definite breaks in certain years rather than secular changes. Semenov and Bengtsson (2002), analyzing global ECHAM4 data, noted significant negative correlation (about -0.5) between the trend patterns for the shape and scale parameter. They attributed this feature to the correlation between parameter estimators for the Gamma distribution. However, this relatively high correlation is primarily provided by the large-scale (e.g. tropics–extratropics) patterns. Our results over European domain are less influenced by this artifact. Pattern correlations are -0.26 and -0.36 for ERA40 in winter and summer and -0.39 and 0.33 for NCEP1.

In Fig. 9, we show two examples of time series of the scale parameter in the locations of the remarkable summer disagreement of trend estimates in the reanalyses. Time series of the summer scale parameter over Scandinavia (marked by triangles in Figs. 8g,h and 9a) show significant trends of the opposite sign in ERA40 (weak growing tendency of about 0.5 mm/day during 40-year period) and NCEP1 (decrease by 1.2 mm/day during 40 years) data. It is interesting to note also visible discontinuity of the short period interannual to decadal-scale variability in the two precipitation products. Although the correlation coefficient between ERA40 and NCEP1 after the removing the linear trends is significant (0.39), it is not high. Summer changes of the scale parameter in the Alpine region (marked by triangles in Fig. 8g,h) are positive in the NCEP1 (1.4 mm/day during 43 years) and significantly negative in ERA40 (2.8 mm/day during

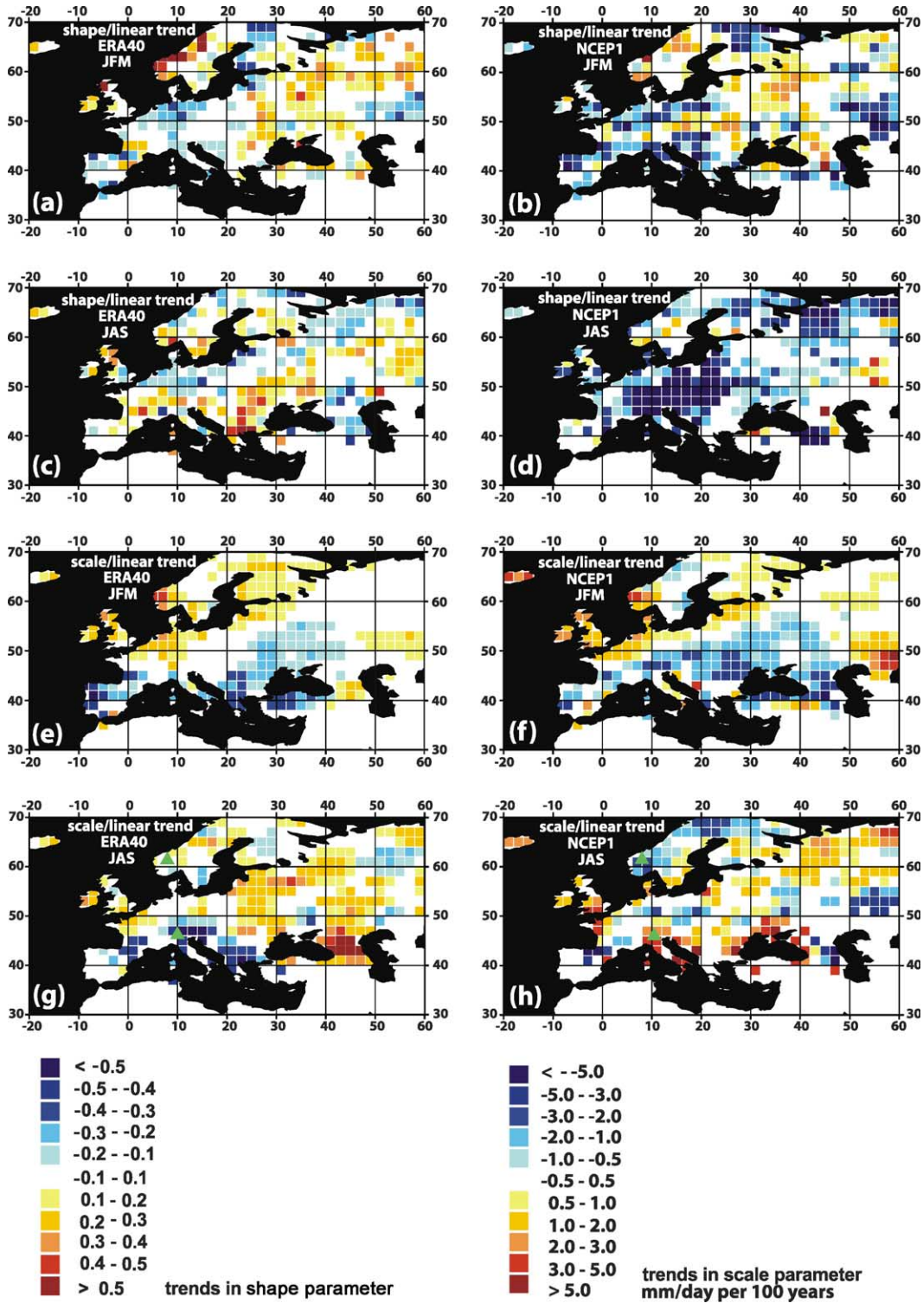
shape/linear trend
ERA40
JFM
(a)
shape/linear trend
NCEP1
JFM
(b)
shape/linear trend
ERA40
JAS
(c)
shape/linear trend
NCEP1
JAS
(d)
scale/linear trend
ERA40
JFM
(e)
scale/linear trend
NCEP1
JFM
(f)
scale/linear trend
ERA40
JAS
(g)
scale/linear trend
NCEP1
JAS
(h)
< -0.5
-0.5 - -0.4
-0.4 - -0.3
-0.3 - -0.2
-0.2 - -0.1
-0.1 - 0.1
0.1 - 0.2
0.2 - 0.3
0.3 - 0.4
0.4 - 0.5
> 0.5
trends in shape parameter
< - -5.0
-5.0 - -3.0
-3.0 - -2.0
-2.0 - -1.0
-1.0 - -0.5
-0.5 - 0.5
0.5 - 1.0
1.0 - 2.0
2.0 - 3.0
3.0 - 5.0
> 5.0
trends in scale parameter
mm/day per 100 years

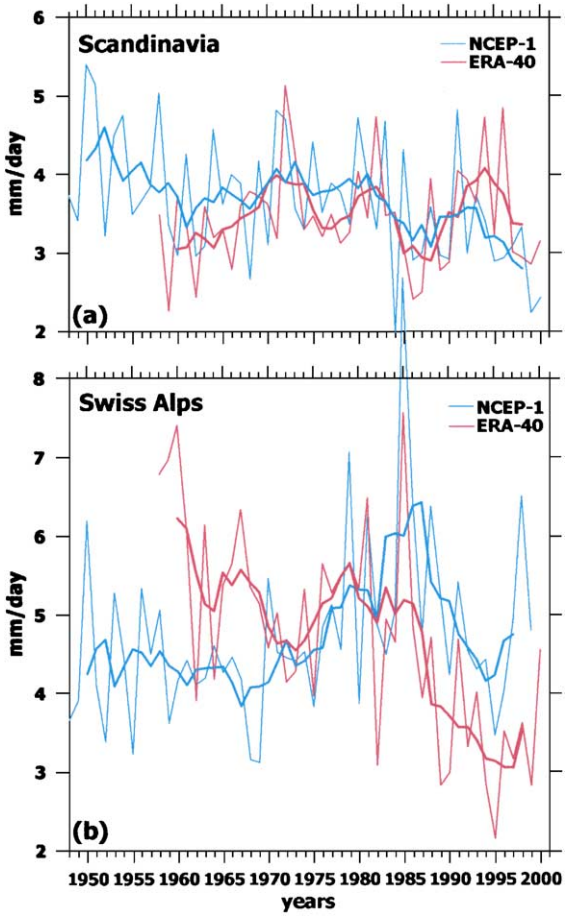

Fig. 9. Time series of the summer scale parameter in the Scandinavia (a) and in Alpine region (b) (locations are shown in Fig. 8) derived from the NCEP1 and ERA40 reanalyses. Thin lines show seasonal values, thick lines—5-year running mean.

43 years). For these time series, however, one can observe consistent interannual to decadal scale variability in NCEP1 and ERA40 at least after the early 1970s. It is important to note that linear trends in the mean seasonal precipitation and precipitation intensity (not shown here) are quite consistent for both reanalyses, showing qualitatively comparable spatial patterns. Thus, despite consistent secular tendencies in the mean precipitation characteristics, the long-term changes in the characteristics of extreme and heavy rainfall may locally exhibit different results for the ERA40 and NCEP1 reanalyses.

Fig. 10 shows correlations between the de-trended anomalies of the shape and scale parameters derived from the NCEP1 and ERA40 reanalyses for the period of overlap. During winter, correlation for the shape parameter is higher than 0.5 in Northwestern Europe, along the main storm track area in the Eastern Europe. Over the Northeastern and Southern Europe correlation decreases, frequently below the significance level (95% significance is slightly higher than 0.3 for time series analyzed). In summer, we observe a much lower level of correlation everywhere, first of all in Central and Southern Europe. For the scale parameter (Fig. 10b,d) in winter, a continuous pattern of very high correlation (above 0.7) is observed over the most European regions, except for the Mediterranean coast. In summer, correlation higher than 0.5 is only observed in Scandinavia, British Islands and Northeastern Europe. Thus, we can conclude that in winter, when parameters of Gamma distribution are largely influenced by the large-scale patterns of the stratiform precipitation, different NWP products are relatively highly correlated with each other, especially for the scale parameter. Considerable drop of correlation between different NWP precipitation products for the parameters of Gamma distribution in summer can be explained by the impact of the mesoscale convective precipitation, whose role largely increases during summer season.

We can hypothesize that at least in winter the changes in the parameters of Gamma distribution should be linked to the NAO index. Heavy precipitation should be associated with intense cyclones, which show close links to the NAO index in the Atlantic-European sector (Gulev et al., 2001, 2002) along with the SLP and mean precipitation (e.g. Hurrell and van Loon, 1997; Maechel et al., 1998). We computed correlations between the NAO index and scale and shape parameters for the four data sets. We used for this purpose the NAO index based on Reykjavik and Ponta Delgada (Hurrell, 1995) to keep it independent on reanalyses. Different reanalyses show qualitatively very comparable projections of the

Fig. 8. Linear trends in the shape parameter (per 100 years; a, b, c, d) and scale parameter (mm/day per 100 years; e, f, g, h) derived from ERA40 (a, c, e, g) and NCEP1 (b, d, f, h) reanalyses for winter (a, b, e, f) and summer (c, d, g, h) for the period 1958–2001. Areas, where trends are insignificant at 95% level (Student's *t*-test) are blanked.

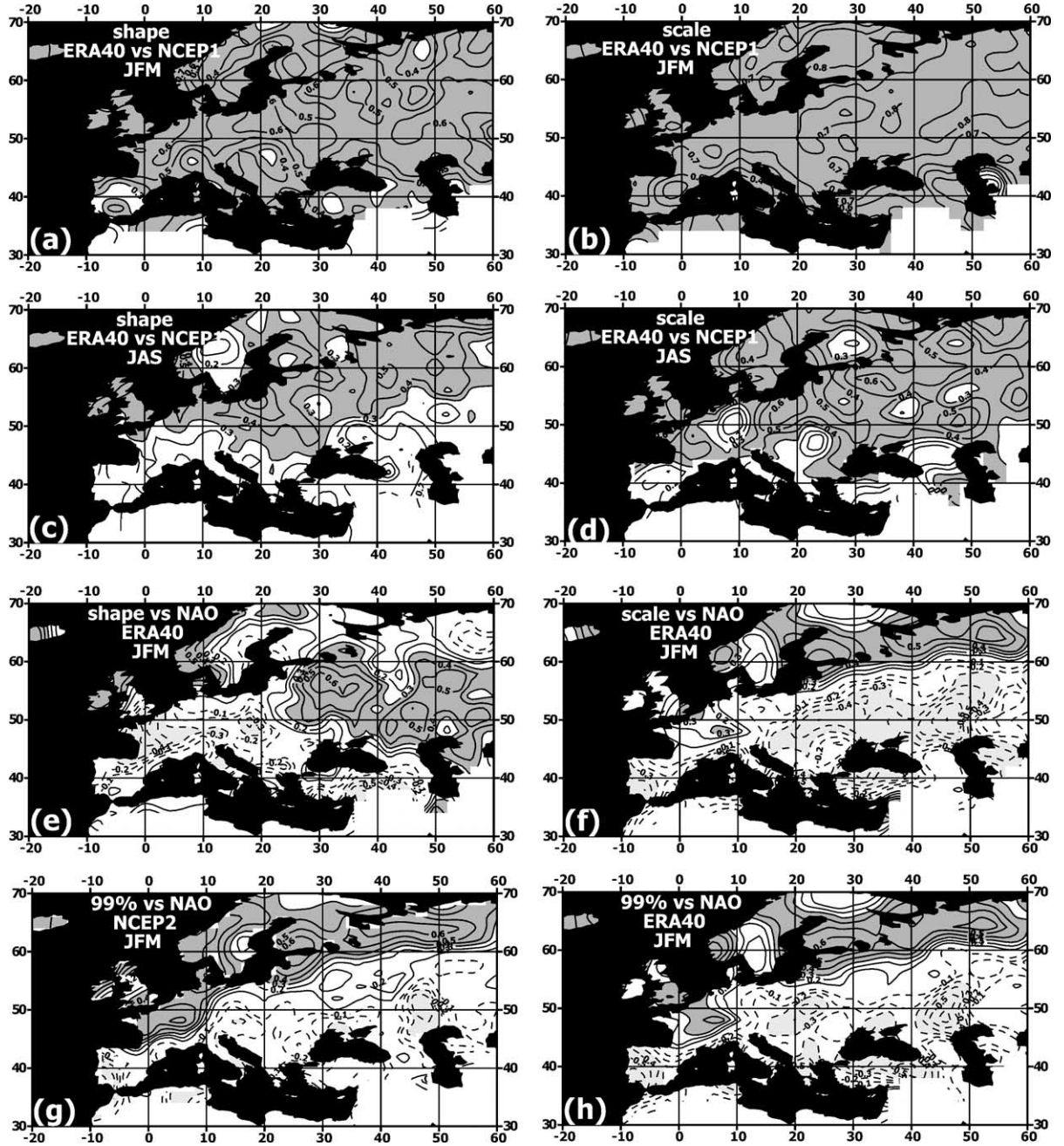

Fig. 10. Correlations between the de-trended anomalies of the shape (a, c) and scale (b, d) parameters derived from the NCEP1 and ERA40 reanalyses for the period 1958–2001 for winter (a, b) and summer (c, d), associated correlation for the winter season between the NAO index and shape parameter (e) as well as between the NAO index and scale parameter (f) for the period 1979–1993, derived from ERA40 reanalysis, and associated correlation between the NAO index and 99% percentile of precipitation in NCEP2 (g) and ERA40 (h). Areas of significant correlation are shaded.

NAO onto the heavy precipitation characteristics. Fig. 10e,f shows associated correlations for the winter season derived for the period 1979–1993 from ERA40 reanalyses data, which indicate the highest correlation level. Associated correlation pattern for the shape parameter is represented by a Northeast–Southwest dipole, which is very robust in all four reanalyses. NCEP2 shows correlation values which are very close to those diagnosed by ERA40. ERA15 and NCEP1 show 5% to 10% weaker correlation in comparison to ERA40. The NAO correlation with the scale parameter is also qualitatively consistent between the data sets, showing Northwest–Southeast dipole-like patterns with positive correlations in the Northern Europe and negative correlations in the Southern and Eastern Europe. The actual values of the correlation coefficients between the NAO and the scale parameter are very close to each other in all four products, varying from each other within 0.05. NCEP2 reanalysis shows slightly weaker negative correlation than the other products in the Southeastern Europe. Analysis on longer time series for 44 years (ERA40) and 54 years (NCEP1) reveals correlation patterns similar to those for 1979–1993 with somewhat smaller (10 to 15%) level of correlation. We performed similar analysis for the shape and scale parameters, derived from the time series without ad hoc correction (elimination of small precipitation less than 0.1 mm/day; not shown). For both correlation between different reanalyses and NAO projections, it holds the same correlation patterns, but gives 5% to 15% higher values of correlation coefficients. When the small precipitation values are not eliminated, NCEP products show the strongest positive correlations with the NAO index, and ECMWF products show the weakest correlation. The NAO projections onto the variability in the intensity of heavy and extreme precipitation show the patterns which closely follow those for the scale parameter. Fig. 10g,h shows associated correlation between the NAO index and 99% percentile precipitation in NCEP2 (Fig. 10g) and ERA40 (Fig. 10h). Associated correlation patterns for 99% precipitation values are qualitatively comparable with those diagnosed for the scale parameter. However, they show stronger positive correlation in the Northern European regions and a weaker negative correlation in the Southeastern Europe. NCEP2 shows somewhat higher than ERA40 positive correlation with NAO over the Northern Europe and Scandinavia.

EOF analysis of the de-trended anomalies of the scale and shape parameters in different reanalyses for the period of overlap (1979–1993; not shown) reasonably demonstrates that the comparability of the winter EOF patterns in the four reanalyses is much higher than for the summer patterns. This is consistent with the results of correlation analysis (Fig. 10a–d) and reflects the fact that statistical characteristics of precipitation in summer are largely dependent on the local conditions and mesoscale precipitation features. For the shape parameter during winter typically the first two EOFs are well separated from each other, explaining 44% to 55% of the total variance, from which 29% to 40% fall on the first EOF and 12% to 17% on the second with the highest percentage observed in the ERA40 and the smallest explained variance diagnosed by ERA40. For the scale parameter in winter the first EOF accounts for 26–34% of total variance and the second for 11–15%. EOF patterns for 99% percentile of the precipitation value are close to those for the scale parameter.

In order to provide an effective intercomparison of interannual variability and to derive patterns of variability in the shape and scale parameters and in the extreme precipitation, which are shared by different precipitation products, we computed the so-called "common EOFs" (Barnett, 1999). For the common EOFs, the partial eigenvalues quantify the relative contribution of the respective data sets to the common eigenmode. When the partial eigenvalue of a particular product shows either a significantly smaller percentage than the other products (the common EOF pattern in this case is dominated by the three other products), or significantly larger percentage than others (the common EOF may exclusively relate to this product), this product can be characterized as an outlier with respect to the others. Fig. 11 shows spatial patterns of the first two common EOFs for the precipitation values corresponding to 99% percentile as well as the first common EOFs for the shape and scale parameters for the winter seasons. Table 2 shows relative partial eigenvalues for these common EOFs. In Fig. 12, we show time series of the normalized principal components (PCs), which characterize the

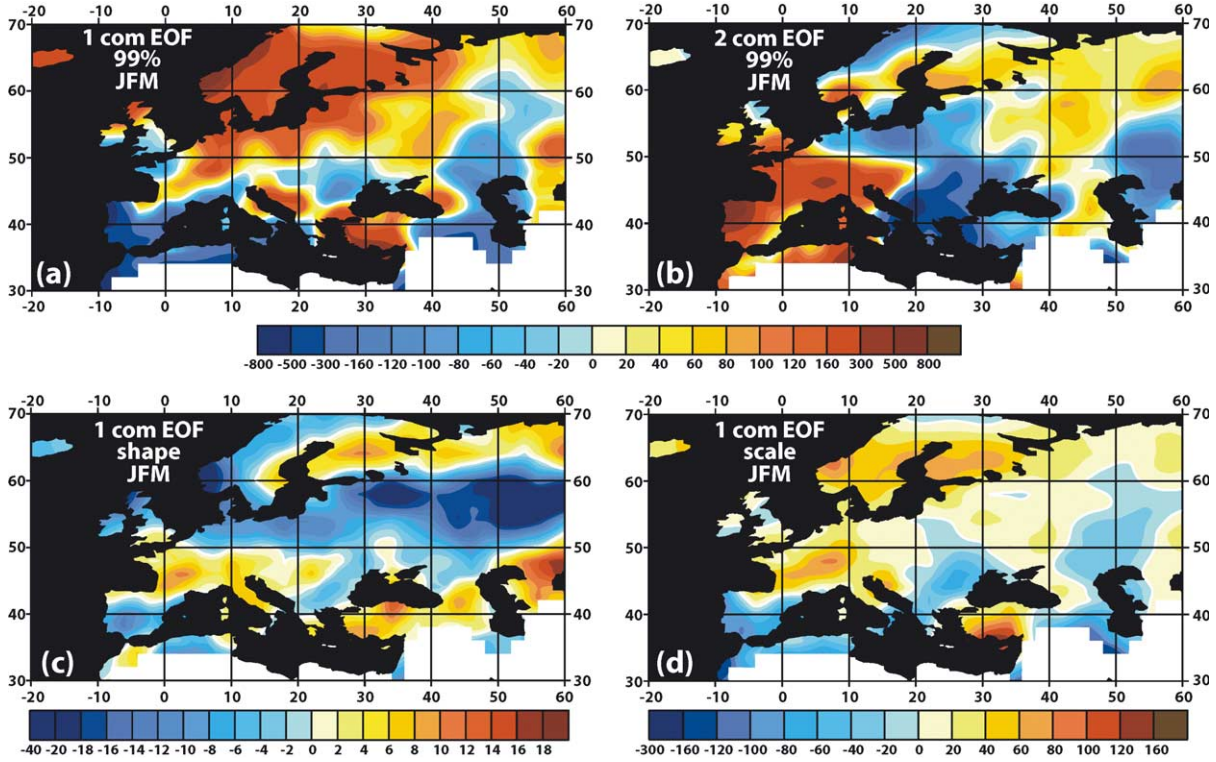

Fig. 11. First (a) and second (b) common EOFs for the 99% precipitation values in winter, as well as the first winter common EOFs of the shape (c) and scale (d) parameters, computed for the period 1979–1993.

changes of the spatial patterns in different reanalyses in time.

The first common EOF in the precipitation corresponding to 99% percentile (29% of the total variance) is shown in Fig. 11a. It shows at least over the western and central European regions a clear dipole structure with the anomalies of the opposite sign over Scandinavia and Northern Europe on one hand and over Southern Europe on the other. Spatial pattern of the second EOF of 99% percentile of precipitation (12% of the total variance) is more complicated and has east–west structure in the Southern and Central Europe and also local maximum of variance along the northern European regions (Fig. 11b). The first common EOF pattern is largely dominated by ERA15 and NCEP2, contributing together about 70% to this mode (Table 2), while the contribution from ERA40 and ERA15 is smaller. The second mode is equally shared by different products with somewhat higher contribution from ERA15 and somewhat smaller percentage for ERA40. The temporal behaviour of the normalized principal components (Fig. 12a,b) is generally consistent in all four reanalyses for the first and the second leading modes. ERA15 PCs exhibit minor deviations from the other reanalyses in the early and mid-1980s. The first leading common mode of the shape parameter in winter (27% of the total variance) exhibits a zonal tripole structure (Fig. 11c). ERA40 dominates in this pattern, contributing 34%. ERA15 and NCEP1

Table 2
Relative partial eigenvalues (%) for the leading modes of the common EOFs of the shape parameter for different reanalyses for the winter (JFM) and summer (JAS) seasons

Reanalyses	First common leading mode			Second common leading mode
	99% percentile	Shape	Scale	99% percentile
ERA15	32.9	24.5	23.8	28.9
ERA40	12.0	33.6	14.4	21.1
NCEP1	18.9	25.4	24.0	25.4
NCEP2	36.2	16.5	37.8	24.6

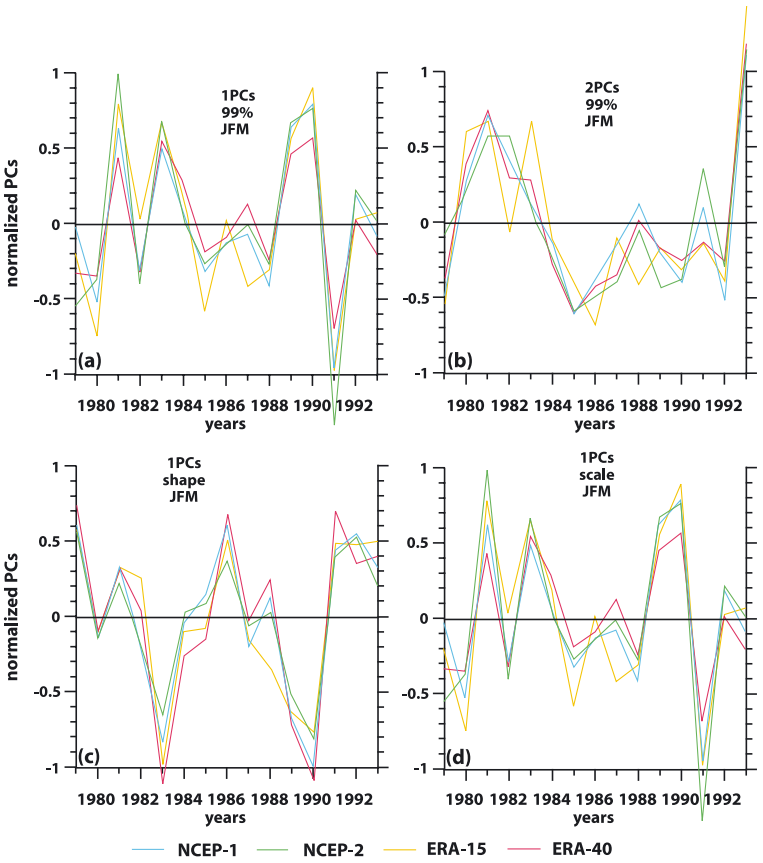

Fig. 12. Time series of the first (a) and second (b) normalized principal components for the 99% precipitation values as well as of the first principal components for the shape parameter (c) and scale parameter (d), derived from different reanalyses for 1979–1993.

equally contribute about 25% and NCEP2 contributes 16% to this pattern (Table 2). The spatial pattern of the first common EOF of scale parameter (Fig. 11d) is dominated by the maxima of explained variance over Scandinavia and Southern Europe and largely reveals the first common EOF of the 99% percentile of precipitation with minor differences in the Central Europe and over British Islands. Time series of the principal components of the shape parameter shown in Fig. 12c are closely correlated to each other. Contributions of different reanalyses to the first mode of the scale parameter are very close to those for the 99% percentile (Table 2), as well as temporal behaviour of the leading PCs (Fig. 12d). In general, the first common mode of the extreme precipitation (Fig. 11a) has close relations to the first mode of scale parameter, while the second one (Fig. 11b) reminds the first EOF of the shape parameter. Thus, we can hypothesize that most of variability of the extreme precipitation is driven by scale parameter of Gamma distribution. Shape parameter is responsible for the second variability mode. We applied also a canonical correlation analysis (CCA, see e.g. von Storch and Zwiers, 1999) to the extreme (99%) precipitation intensity, shape and scale parameters on the basis of individual reanalyses. Results for at least ECMWF products (no figure shown) clearly demonstrate two canonical pairs, of which the first one is represented by the first EOFs of extreme precipitation and scale parameter and the second one is done by the second EOF of extreme precipitation and the first EOF of the shape parameter.

6. Regional comparison with the station data

6.1. Comparison of the mean statistical characteristics of precipitation

Comparisons of NWP precipitation products with the station data is quite a difficult task, because it should involve the analysis of subgrid-scale precipitation, which is to a different extend accounted for in NWP and station collections (Zolina et al., 2004). Inhomogeneous spatial distribution of station observations and their discrete nature (in contrast, e.g. to reanalyses, which account for convective part of precipitation over grid cell) arise the main problems in performing comprehensive comparison. Having this in mind, we, however, present here a pilot intercomparison of the statistical characteristics of daily precipitation from station data with those derived from different reanalyses. For this comparison, all daily fields from reanalyses were interpolated to the station locations by the method of local procedures (Akima, 1970) and subsampled in order to simulate the missing values inherent in the station data (up to 10% in both KNMI and DWD collections). Fig. 13a,b shows differences in mean precipitation between the stations data and NCEP2 reanalysis, showing primarily the largest values among the other products (Fig. 2). In winter (Fig. 13a), in situ data tend to show primarily higher mean precipitation values in the northern regions and mostly lower than NCEP2 precipitation values over Southern Europe. Differences for the most locations vary within ± 1 mm/day, locally showing strong positive differences (stations larger than reanalysis) over mountain regions. In summer, stations report primarily smaller mean precipitation values with the largest magnitude of differences higher than 3 mm/day in the Central Eastern Europe. Higher values of mean precipitation in station data in comparison to NCEP2 in summer can be frequently observed in the coastal and island locations. This might be an artifact of interpolation procedure and cannot be considered as a natural signal. We have to note that the distribution of differences is largely influenced by small scale spatial inhomogeneity reflecting uncertainties of the validation of NWP data against in situ measurements, mentioned above. The number of wet days is systematically smaller in station data compared to reanalyses (Fig. 13e,f) for both seasons. Differences amount to 15–30% in winter and to 50% in summer with the maxima in the Eastern European regions. As a result, precipitation intensity, derived from the station data, is normally systematically higher than that obtained from reanalyses (Fig. 13c,d). The highest differences, ranging from 0.5 to 2.0 mm/day, are observed in the mountain regions of the Southern Europe. Again, as for the mean precipitation, one can observe impact of the strong spatial inhomogeneity on the pattern of differences, especially pronounced in Central Europe.

Fig. 14a,b shows the differences in the shape parameter, derived from the station data and NCEP2 reanalysis for 15-year period (1979–1993). Note that NCEP2 shows normally smaller shape parameter than ERA40 and in many areas shows the smallest shape factor among all four reanalyses (Fig. 5). In winter, over the Western Europe stations data diagnose smaller skewness of the Gamma distribution with the strongest differences up to 0.4 observed in the southern European regions. In the Eastern Europe stations data give 0.05–0.15 higher shape factor than in NCEP2, that is, however, still smaller than ERA40 values. During summer (Fig. 14b), negative differences in the shape parameter between the stations data and NCEP2 become stronger, increasing to 0.2–0.3 on average and also covering most of the Eastern European regions. Comparison for scale parameter between the stations and NCEP2 (the largest scale factor among four reanalyses) is presented in Fig. 14c,d for winter and summer. In winter, stations report primarily higher values of the scale parameter with differences increasing from 1–2 mm/day in the north to 5–10 mm/day in the Southern Europe. In the Eastern Europe, stations give slightly smaller values with the differences within 1 mm/day. However, in comparison to the other reanalyses station data give higher values also in the Eastern Europe. This patterns also holds in summer (Fig. 14d) with, however, 20–30% stronger positive differences and weaker negative differences in the Eastern Europe (within 0.1–0.3 mm/day). Patterns of differences for the 99% precipitation values (Fig. 14e,f) closely follows that of the scale parameter. Stations exhibit higher values of extreme precipitation by 2 to 5 mm/day in the Central and Eastern Europe to 20–50 mm/day in the Southern Europe.

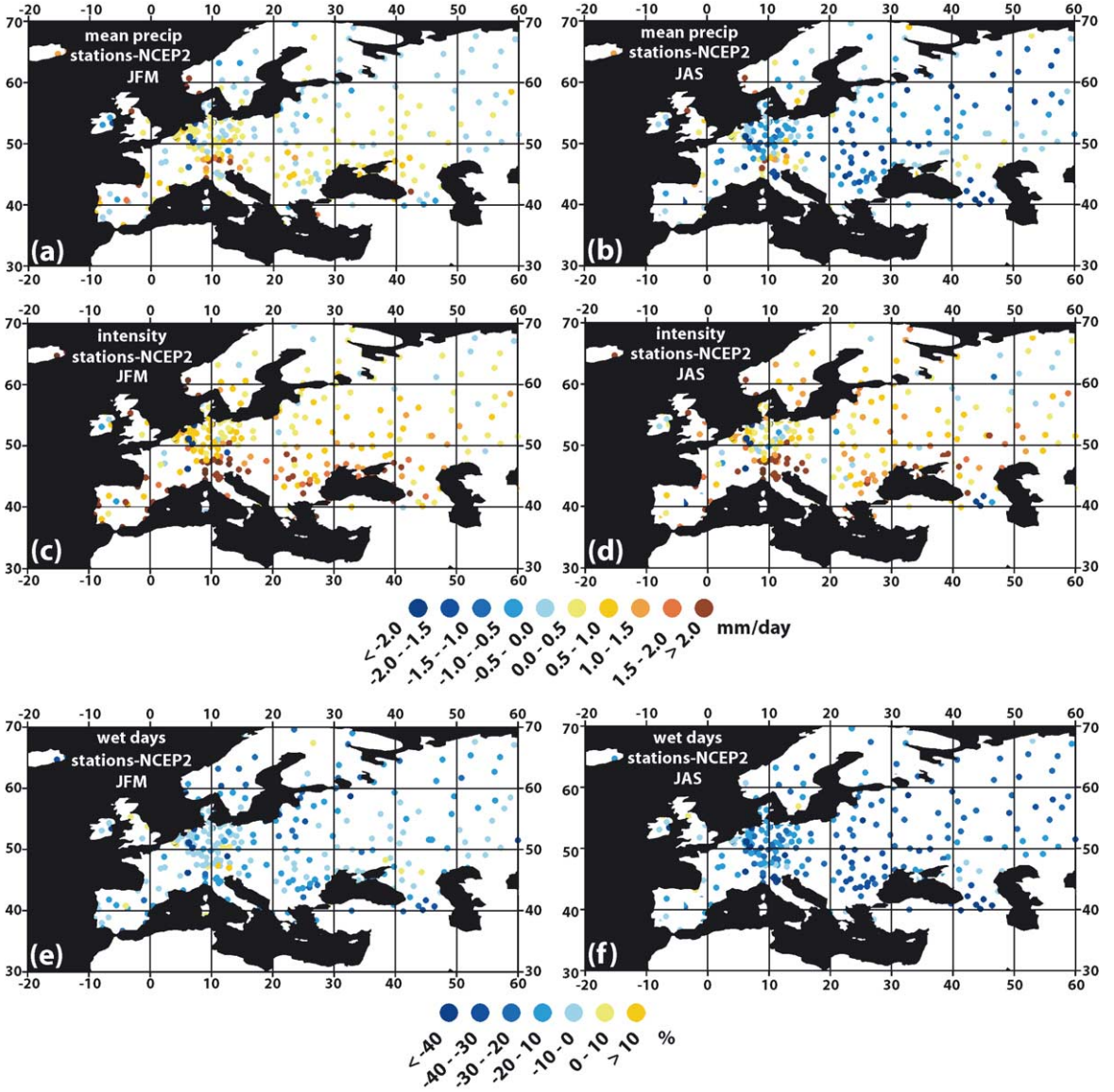

Fig. 13. Differences in the mean precipitation (mm/day), derived from the station data and NCEP2 reanalysis for the period 1979–1993 for winter (a) and summer (b), differences in precipitation intensity (mm/day) between the stations data and NCEP2 for 1979–1993 for winter (c) and summer (d), and differences in the wet days probability between the stations data and NCEP2 reanalysis for 1979–1993 for winter (e) and summer (f).

Table 3 shows synthetic results of comparisons between the station data and four reanalyses for different precipitation characteristics for four regions (Central Europe, Iberian Peninsula, Southeastern Europe and Eastern Russia, Fig. 14g). These regions are characterized by relatively homogeneous spatial coverage of station data. Central Europe and Southeastern Europe provide the highest station density with respect to the other regions. Note that since the reanalyses data were interpolated onto station locations, Table 3 represents area-averaging of station-like sampled reanalyses data and implements the same

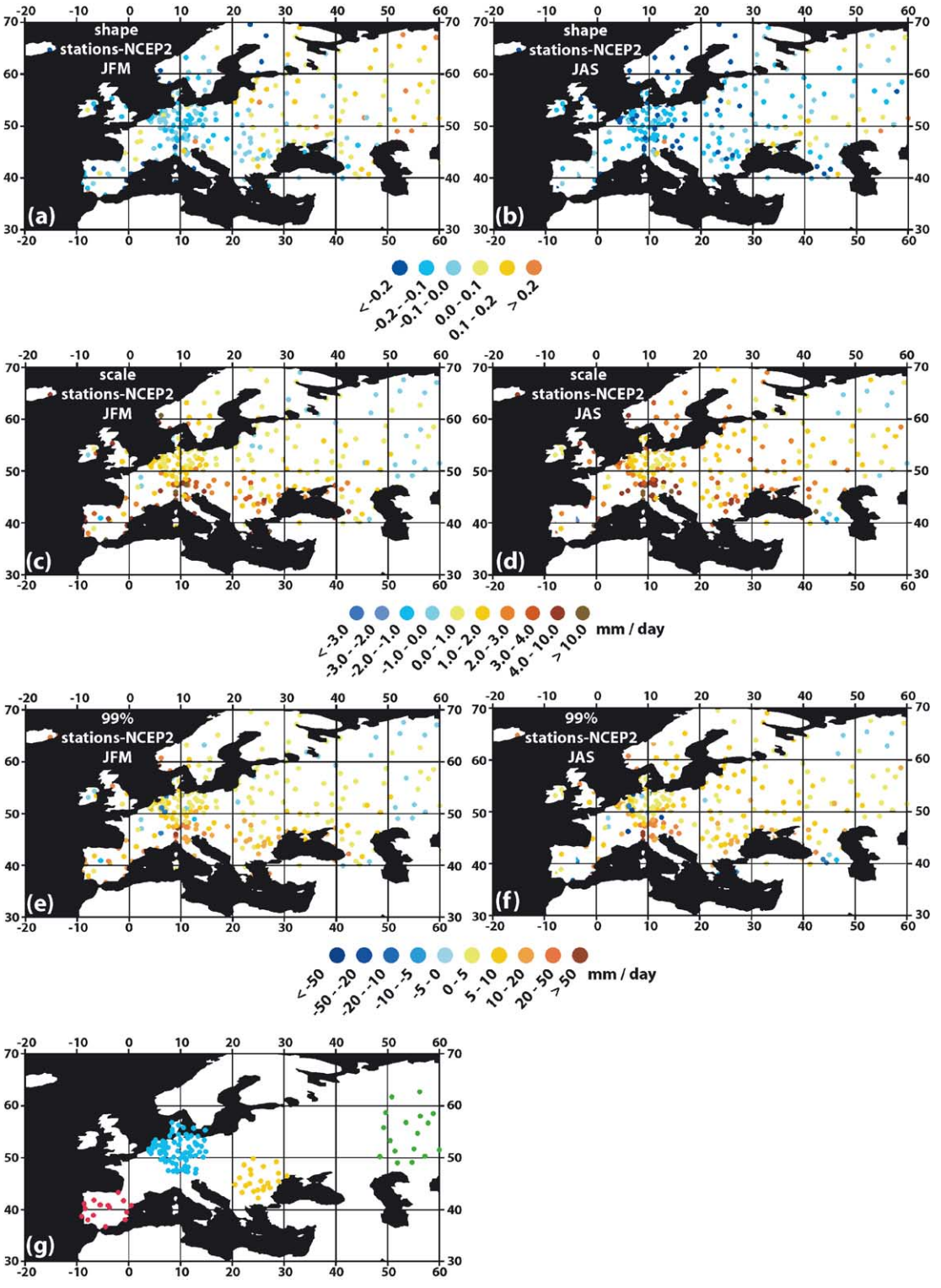
shape
stations-NCEP2
JFM
(a)
shape
stations-NCEP2
JAS
(b)
< -0.2
-0.2 - -0.1
-0.1 - 0.0
0.0 - 0.1
0.1 - 0.2
> 0.2
scale
stations-NCEP2
JFM
(c)
scale
stations-NCEP2
JAS
(d)
< -3.0
-3.0 - -2.0
-2.0 - -1.0
-1.0 - 0.0
0.0 - 1.0
1.0 - 2.0
2.0 - 3.0
3.0 - 4.0
4.0 - 10.0
> 10.0
mm / day
99%
stations-NCEP2
JFM
(e)
99%
stations-NCEP2
JAS
(f)
< -50
-50 - -20
-20 - -10
-10 - -5
-5 - 0
0 - 5
5 - 10
10 - 20
20 - 50
> 50
mm / day
(g)

Table 3
Means (upper numbers) and standard deviations (lower numbers) of statistical parameters of daily precipitation in different European regions for the winter (JFM) and summer (JAS) seasons for the period 1979–1993

	Iberian Peninsula		Central Europe		Southeastern Europe		Eastern Russia	
	JFM	JAS	JFM	JAS	JFM	JAS	JFM	JAS
Mean precipitation (mm/day)								
Stations data	2.0/1.13	0.9/0.71	1.8/0.91	2.3/1.01	1.2/0.27	1.6/0.49	0.9/0.31	1.8/0.85
ERA15	1.5/0.54	0.6/0.36	1.6/0.36	2.1/0.56	0.8/0.09	1.7/0.33	0.7/0.11	1.7/0.71
ERA40	1.3/0.45	0.5/0.21	1.8/0.30	1.7/0.38	1.2/0.08	1.5/0.39	1.1/0.13	1.5/0.62
NCEP1	1.5/0.41	1.0/0.55	1.6/0.52	2.7/0.64	1.2/0.18	2.9/0.51	0.9/0.22	2.3/1.19
NCEP2	1.5/0.49	1.4/0.73	1.4/0.35	2.6/0.48	0.9/0.15	3.0/0.41	0.9/0.17	2.6/0.90
Wet days probability (%)								
Station data	33/10	16/11	52/9	45/8	36/9	27/8	45/14	37/17
ERA15	50/9	28/11	70/7	76/4	54/5	59/7	48/6	59/13
ERA40	53/8	33/9	73/4	68/4	64/6	64/8	68/6	62/14
NCEP1	46/6	28/11	66/8	66/7	61/7	60/7	61/10	56/18
NCEP2	43/5	28/9	59/4	61/3	48/5	57/6	55/9	61/15
Precipitation intensity (mm/day)								
Stations data	5.8/1.94	5.5/1.60	3.5/1.48	5.1/1.61	3.5/0.82	6.0/0.63	2.0/0.38	4.6/0.79
ERA15	2.9/1.02	2.1/0.40	2.3/0.48	2.9/0.62	1.5/0.23	2.8/0.28	1.5/0.14	2.7/0.49
ERA40	2.4/0.73	1.5/0.34	2.4/0.42	2.4/0.49	1.8/0.20	2.4/0.35	1.7/0.15	2.3/0.50
NCEP1	3.1/0.81	3.4/0.67	2.3/0.54	4.0/0.81	1.9/0.33	4.9/0.44	1.5/0.22	3.6/1.02
NCEP2	3.6/0.76	4.5/1.04	2.4/0.47	4.2/0.57	2.0/0.32	5.1/0.39	1.6/0.12	4.1/0.93
Precipitation of 99% percentile (mm/day)								
Stations data	34.2/12.2	35.8/12.7	18.1/8.2	28.1/8.9	19.1/6.1	34.0/4.3	9.3/2.4	23.9/4.5
ERA15	16.8/8.1	11.7/2.8	10.9/2.4	14.6/3.2	7.8/1.5	15.0/1.4	6.4/0.8	13.6/2.3
ERA40	12.6/4.1	7.9/2.0	11.5/2.1	11.9/2.7	9.3/1.4	11.6/1.7	7.6/0.9	11.2/2.0
NCEP1	16.2/4.4	19.1/3.7	11.2/2.5	18.8/3.9	10.2/2.1	24.4/2.7	7.1/1.1	17.1/4.1
NCEP2	18.9/5.1	25.5/8.1	12.1/2.4	21.0/3.2	10.8/2.5	26.8/3.5	8.0/0.8	20.6/3.7
Shape parameter								
Station data	0.65/0.11	0.54/0.09	0.78/0.08	0.71/0.08	0.72/0.11	0.66/0.08	1.01/0.11	0.79/0.09
ERA15	0.69/0.08	0.68/0.09	0.92/0.05	0.84/0.05	0.82/0.08	0.76/0.05	0.96/0.06	0.83/0.05
ERA40	0.78/0.06	0.73/0.04	0.96/0.03	0.90/0.04	0.85/0.09	0.88/0.06	1.04/0.08	0.92/0.07
NCEP1	0.77/0.05	0.69/0.04	0.90/0.04	0.95/0.05	0.77/0.08	0.84/0.06	0.88/0.10	0.89/0.10
NCEP2	0.76/0.03	0.68/0.03	0.86/0.04	0.86/0.04	0.74/0.07	0.77/0.05	0.90/0.07	0.81/0.09
Scale parameter, mm/day								
Station data	9.1/3.51	10.2/4.2	4.4/2.1	7.1/2.30	4.8/1.42	8.8/0.96	2.0/0.55	5.8/1.16
ERA15	4.4/2.22	3.0/0.84	2.4/0.60	3.4/0.78	1.9/0.44	3.7/0.38	1.4/0.24	3.2/0.56
ERA40	3.1/1.1	2.0/0.51	2.5/0.52	2.7/0.70	2.2/0.41	2.7/0.40	1.6/0.27	2.5/0.44
NCEP1	3.9/1.3	4.9/0.95	2.5/0.56	4.1/0.81	2.5/0.59	5.7/0.56	1.6/0.30	3.9/0.84
NCEP2	4.6/1.2	6.5/2.0	2.8/0.60	4.8/0.77	2.7/0.70	6.5/0.72	1.8/0.26	4.9/0.67

area-weighting as the station data do. Thus, it can be mostly used for the comparative assessments rather than be interpreted as regional estimates from reanalyses. In winter, mean precipitation derived from the stations data is normally higher than that computed from most of reanalyses everywhere, except

Fig. 14. Differences in the shape parameter, derived from the station data and NCEP2 reanalysis for the period 1979–1993 for winter (a) and summer (b), differences in the scale parameter (mm/day), derived from the station data and NCEP2 reanalysis for the period 1979–1993 for winter (c) and summer (d), and differences in the 99% precipitation values (mm/day), derived from the station data and NCEP2 reanalysis for the period 1979–1993 for winter (e) and summer (f); (g) shows the arrangement of stations for the four regions intercompared in Table 3.

for Eastern Russia. In summer, stations' estimates of mean precipitation are lying within the range of values derived from the reanalyses. Stations data report considerably smaller probability of wet days with the strongest relative differences over Iberian Peninsula and Southeastern Europe, where reanalyses give 1.3 to 1.7 times higher frequency of wet days in winter and up to 2.1 times more wet days in summer. Precipitation intensity is considerably higher when derived from the station data with the largest differences in the Southeastern Europe. Scale parameter as well as precipitation values, corresponding to 99% percentile, derived from the station data, are two to more than three times larger than in the reanalyses with the highest relative differences over Iberian Peninsula and Southeastern Europe in summer. The shape parameter is normally somewhat smaller in the station data than in reanalyses except for the Eastern Russia, where stations report higher shape parameter in winter.

Quantitative regional differences between the station data and reanalyses should be considered in the context of standard deviations (std) of estimates also given in Table 3 for the four regions. For the characteristics of heavy and extreme precipitation (99% percentile) as well as for the parameters of Gamma distribution and precipitation intensity, differences between the station data and reanalyses can be considered as statistically significant. Besides this, standard deviations of estimates in Table 3 show that normally stations data are characterized by much stronger spatial variability than the reanalyses data, showing higher std values. This shows that the comparison of statistical characteristics derived from the station data and from NWP products is largely influenced by mesoscale variability. It is interesting to note that in the Eastern Russia std estimates derived from stations and reanalyses become much closer to each other and that reanalyses can show even higher std values that is not the case for the other regions. However, in this region, station density is considerably smaller than in the others. Such a separation cannot as effectively account for the mesoscale spatial variability in precipitation characteristics, as in the other regions, characterized by much higher station density. Moreover, the magnitude of mesoscale spatial variability itself is considerably smaller in the Eastern Russia than in Western European regions. Thus, standard deviations derived from both stations data and reanalyses in this region to a higher extent account for large-scale spatial variability than for the mesoscale features.

6.2. Interannual variability of the statistical characteristics of daily precipitation in station data and reanalyses

In Fig. 15, we show correlation between the detrended anomalies of the shape (Fig. 15a,b) and scale (Fig. 15c,d) parameters, derived from the station data and ERA40 reanalysis for winter (Fig. 15a,c) and summer (Fig. 15b,d). Note that the pattern of correlation for the precipitation corresponding to 99% percentile (not shown) is very close to that for the scale parameter. Anomalies of the scale parameter are considerably strongly correlated in the station data and in reanalyses, than the anomalies of the shape parameter. Winter correlation between the station data and reanalysis is 20% to 30% higher than that observed in summer. For the shape parameter, correlation exceeds 0.5 in 32% of points in winter and in only 14% of locations in summer. At the same time for the scale parameter in winter, 62% of points show the correlation higher than 0.5 and about 26% of points indicate correlation higher than 0.7. During summer for the scale parameter, correlation higher than 0.5 is observed in 32% of locations and correlation higher than 0.7 is identified in less than 15% of points. This is in agreement with the strong impact of regional mesoscale variability on interannual variability during summer, mentioned above. The largest correlation during both seasons is observed over the Northeastern and Eastern Europe and the smallest in the Southern Europe and mountain regions, where the impact of spatial inhomogeneity considerably increases.

For two locations (Bulken, 60.7N, 6.2E and Porto, 41.1N, 8.6W), we performed a pilot intercomparison of statistical characteristics of precipitation in ERA40 and NCEP1 with those computed on the basis of stations data from KNMI collections. The two locations in Scandinavia and on Iberian Peninsula are characterized by the pronounced changes of characteristics of heavy precipitation and also indicate comparability between ERA and NCEP reanalyses. In order to perform the comparison, we derived from the

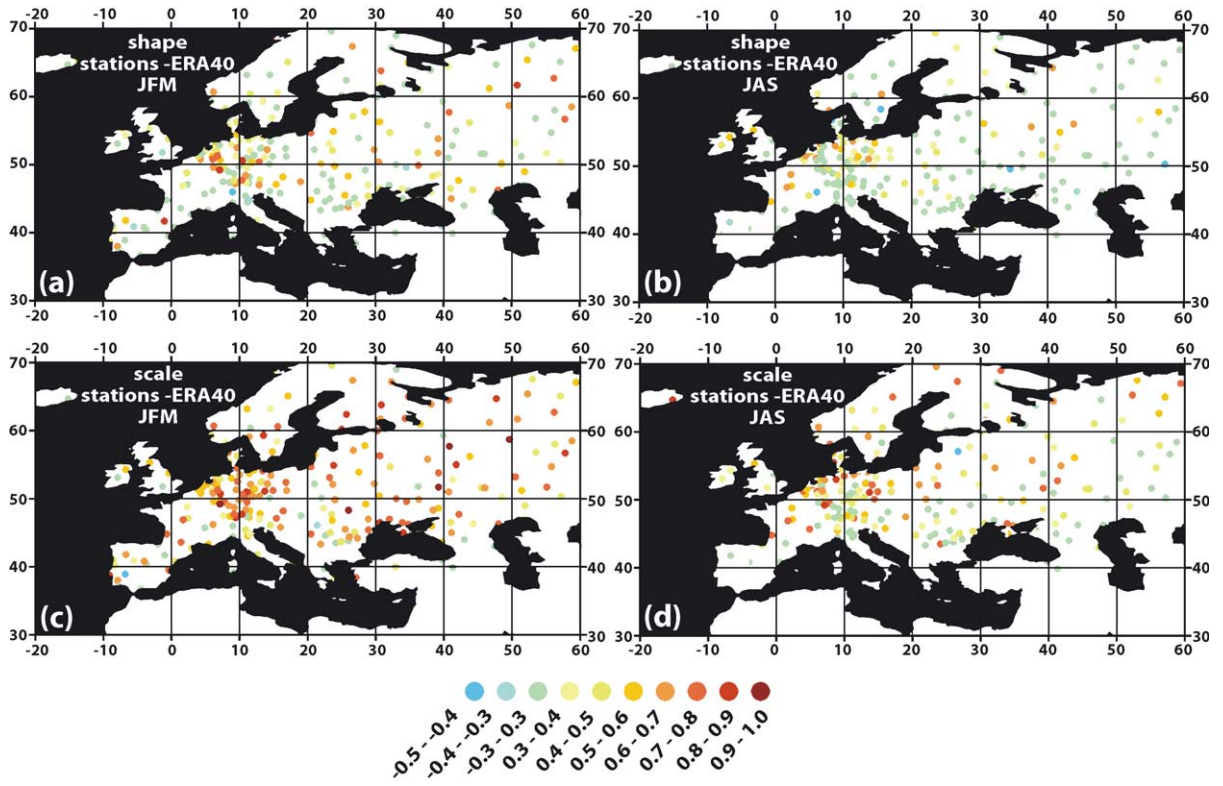

Fig. 15. Correlation between the de-trended anomalies of the shape (a, b) and scale (c, d) parameters, derived from the station data and ERA40 reanalysis for winter (a, c) and summer (b, d).

station and reanalyses data what we term the occurrence anomalies. For every time series, we computed PDFs of daily precipitation for individual seasons. Averaging of these PDFs over years gives the time-averaged PDFs, which are reasonably close to those obtained by analyzing all data for the whole observational period. Then we derived PDF anomalies for individual years for particular classes by subtracting the mean PDF from those for the calendar years and normalized them by scaling with the interannual standard deviations (std) of the frequency for the selected bins:

$$P'(x) = [P(x) - \langle P(x)\rangle]/\sigma[P(x)], \qquad (2)$$

where x is the percentile of the daily precipitation, $P(x)$ is the probability density distribution for an individual season, $P'(x)$ is the normalized anomaly of the probability density distribution, and $\langle\rangle$ is the averaging operator. We used earlier the occurrence anomalies for the analysis of changes in cyclone life cycle (Gulev et al., 2001). Gershunov (1998) analyzed in somewhat more simplified manner differences in the precipitation PDFs for different years over the United States. Figs. 16 and 17 show the temporal evolution of the probability density function in the two locations in winter and summer, smoothed with 3-year running mean. In winter in the Northern Europe (Norway), there is a clear growing tendency in the occurrence of extreme and heavy precipitation (70% and higher percentiles) and the decrease in occurrence of small precipitation associated with the classes 0–30%. These features are clearly pronounced in all three data sets. For the classes from 30% to 70%, one can find less consistency in the temporal evolution of PDFs. The opposite conclusion can be drawn from the analysis of winter diagrams for Iberian Peninsula (Fig. 17). Growing probability of small precipitation goes along with the decreasing occurrence of precipitation for the higher percentiles. In 1979, we can identify an abrupt change in the diagram for NCEP1. Qualita-

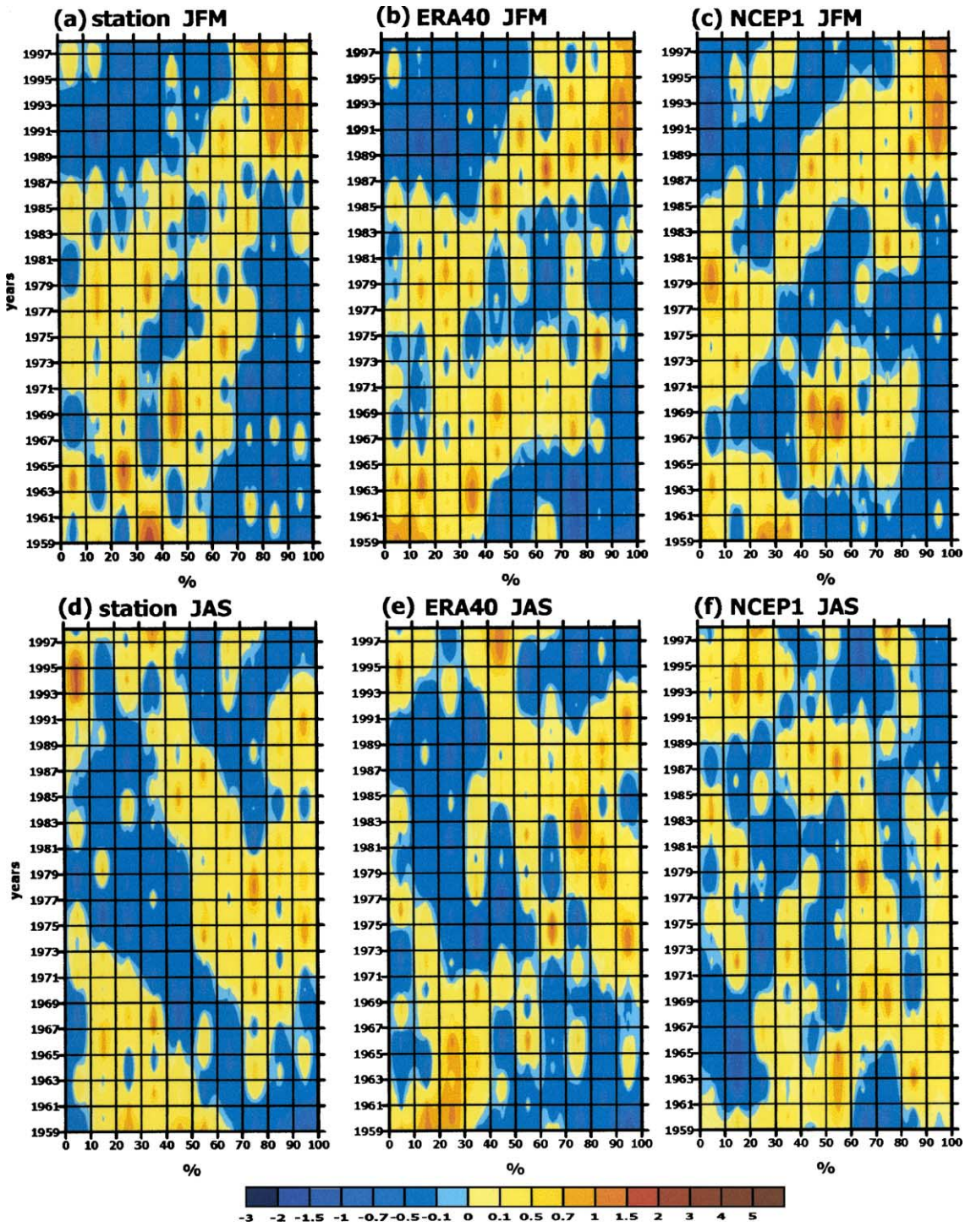

Fig. 16. Temporal evolution of the probability density function in the Northern Europe (Norway, Bulken, 60.7N, 6.2E) in winter (a, b, c) and summer (d, e, f), smoothed with 3-year running mean, derived from station data (a, d), ERA40 (b, e) and NCEP1 (c, f).

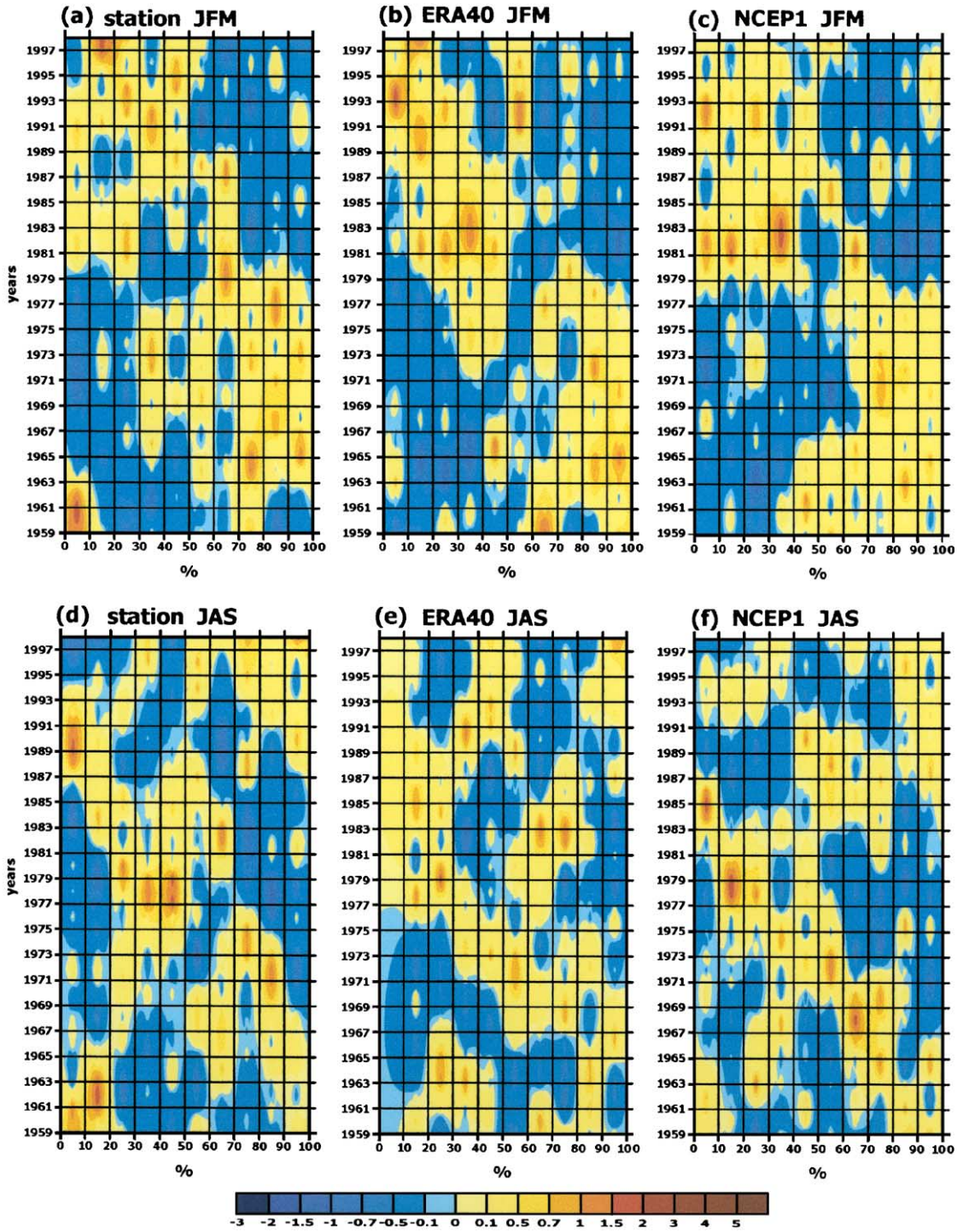

Fig. 17. Same as in Fig. 16, but for Iberian Peninsula (Porto, 41.1N, 8.6W).

tively comparable variability patterns for the heavy and weak precipitation classes are superimposed by the inconsistency between the two reanalyses and station data changes in the range of moderate precipitation.

In summer for the location in Norway (Fig. 16), the two reanalyses show a little comparability in the PDF changes for most classes. Station data exhibit some consistency with ERA40 at least for the classes corresponding to the weak and heavy precipitation. Basically the same peculiarities can be reported for Iberian Peninsula in summer season: strong weakening of the consistency of the PDF variability in reanalyses and station data (Fig. 17). Thus, reanalyses demonstrate acceptable skills in the simulation of the variability of heavy and extreme precipitation in cold season. However, this does not guarantee necessarily an adequate simulation of the actual values of precipitation extremes, as it has been pointed out above.

7. Summary and discussion

We analyzed statistical characteristics of European precipitation on the basis of four reanalyses data sets, widely used in climate studies and found remarkable differences in the shape and scale parameters of Gamma distribution of daily precipitation, as well as extreme precipitation values. In general, NCEP products show higher values of extreme precipitation than ECMWF products. NCEP2 shows the highest estimates of precipitation extremes and ERA15 gives the smallest ones. The estimation of extremes in terms of long-term return values or return periods (e.g. Hennessy et al., 1997) will result in higher precipitation extremes, especially in summer, in NCEP products in comparison to ERA products and in NCEP2 compared to NCEP1. The diagnosed differences in the characteristics of Gamma distribution (shape and scale parameters) and extreme precipitation values between different NWP products may vary within 30–40% on average. This is larger than the differences in these characteristics simulated by climate models in greenhouse gas experiments (Hennessy et al., 1997; Semenov and Bengtsson, 2002), which report normally the largest changes between the greenhouse gas experiments and the present climate to be within 10% to 20%. Thus, one has to be careful when choosing reanalysis data set for the description of what we term the present climate.

Secular tendencies in statistical characteristics of daily precipitation in ECMWF and NCEP reanalyses, showing qualitatively comparable patterns in winter, may locally exhibit significant differences in summer, in particular in the Southern Europe. The correlation between NCEP and ECMWF for the parameters of Gamma distribution and extreme precipitation is much stronger in winter, dominated by large-scale patterns (e.g. NAO) than in summer, largely influenced by the impact of regional effects of mesoscale nature. Interannual variability in the extreme precipitation analyzed using common EOFs shows that the first commonly shared pattern is driven by the leading mode of variability in the scale parameter. Second-order mode of the variability of precipitation extremes is associated with the leading mode of the variability of shape parameter.

Comparison of precipitation statistics from reanalyses with observations is largely influenced by spatial inhomogeneity of station data and local impacts of mesoscale processes. This effect affects both comparisons of means and interannual variability patterns, especially in summer. Nevertheless, to the extent that it is possible to make comparative assessment using these very different data sources (NWP and stations), we can draw the conclusion that characteristics of extreme precipitation over Europe in NCEP products (especially NCEP2) are closer to the stations data than those of ECMWF products. However, this conclusion should be considered with caution and does not mean that precipitation in NCEP products is superior with respect to ERA in all other respects, such as global hydrological cycle characteristics, precipitation over oceans and others.

Considering reanalyses, differences in model parameterizations, spatial resolution and data assimilation input can be responsible for the differences observed. In ERA15 and ERA40 reanalyses, precipitation parameterizations were run on a finer reduced Gaussian grid than in NCEP1 and NCEP2 reanalyses. However, the observed differences (in particular, higher extreme precipitation in NCEP products) should be likely attributed to the performance of parameterizations and data assimilation input. Assimilation of Xie and Arkin (1997) pentadal rainfall from

1980s in NCEP2 resulted in the increase of extreme precipitation values in this product in comparison to NCEP1. At the same time, NCEP1 demonstrates much stronger than NCEP1 spatial inhomogeneity of precipitation characteristics due to a smoother topography used in NCEP2 (Kanamitsu et al., 2002). Note that for this comparison we excluded from reanalyses daily precipitation values smaller than 0.1 mm/day. This ad hoc correction increase the shape parameter and decrease the scale parameter in the most locations, having the larger impact on ERA40 and NCEP2 reanalyses. These very small precipitation values are primarily associated with the stratiform component.

Regional differences in the long-term tendencies of statistical characteristics of precipitation are associated with the changes in data assimilation input in different reanalyses (first of all VTPR and TOVS in ERA40 after 1972). Note that NCEP2 and NCEP1 show comparable secular tendencies (not shown here). Thus, assimilation of Xie and Arkin (1997) pentadal rainfall changing mean characteristics did not implement any new linear trends in NCEP2 compared to NCEP1. This allows for the consideration of secular changes found in NCEP1 as quite reliable.

Further validation efforts should be focused on the detailed comparison of statistical characteristics of precipitation from reanalyses with station data. This comparison should involve analysis of mesoscale spatial variability and its impact on estimates of statistical characteristics (Osborn and Hulme, 1997). On one hand, real orography, reflected by the station data, forces a much stronger spatial inhomogeneity in the mesoscale precipitation patterns, than in reanalyses (e.g. Booij, 2002). On the other hand, inhomogeneous arrangement of stations does not adequately sample the orography, while NWP products do (if only a smoothed one). Using the method of Zolina et al. (2004), we can quantitatively estimate the subgrid-scale component of precipitation in the well-sampled regions. However, due to the different saturation of stations in different European regions, we do expect serious changes in the effectiveness of quantification of the mesoscale part from one region to another. Nevertheless, our comparison implies considerable underestimation of the heavy and extreme rainfalls in reanalyses products. Since the difference between statistical characteristics derived from the station data and from reanalyses is of the same order of magnitude or higher than the variations between different reanalyses, we can conclude that these deviations represent a robust signature. At the same time, temporal variations of the occurrence of extremes can be quite effectively diagnosed by reanalyses, at least in comparison to the moderate precipitation.

Acknowledgements

This study is supported by the North Rhine-Westphalia Academy of Science under the project "Large Scale Climate Changes and their Environmental Relevance". We greatly appreciate suggestions and criticism of anonymous reviewers, whose contribution to the improvement of the manuscript was tremendous. We also appreciate discussions with Pavel Groismann of NCDC (Asheville), Andreas Hense of MIUB (Bonn) and Vladimir Semenov of IFM (Kiel) and reliable editorial assistance of Martin Beniston of Fribourg University. NCEP reanalyses were made available by courtesy of NCEP and ERA reanalyses were provided by ECMWF and German Weather Service (DWD). DWD is also acknowledged for the provision of station data over Germany. We also benefited from the support of Russian Foundation for Basic Research (Grant 02-56331).

References

Akima, H., 1970. A new method of interpolation and smooth curve fitting based on local procedures. ACM J. 17, 589–602.

Arpe, K., Klepp, C., Rhodin, A., 1999. Differences in the hydrological cycles from different reanalyses—which one shall we believe? Proc. Conf. 2nd Intl. Conf. on Reanalyses, Reading, England, 23–27 Aug, WCRP vol. 109. WMO, Geneva, pp. 193–196. WMO/TD 985.

Barnett, T.P., 1999. Comparison of near surface air temperature variability in 11 coupled global climate models. J. Climate 12, 511–518.

Beniston, M., 1997. Variations of snow depth and duration in the Swiss Alps over the last 50 years: links to changes in large-scale climatic forcing. Clim. Change 36, 281–300.

Beniston, M., Rebetez, M., Giorgi, F., Marinucci, M.R., 1994. An analysis of regional climate change in Switzerland. Theor. Appl. Climatol. 49, 135–159.

Booij, M.J., 2002. Extreme daily precipitation in Western Europe with climate change at appropriate spatial scales. Int. J. Climatol. 22, 51–69.

Corte-Real, J., Qian, B., Xu, H., 1998. Regional climate change in Portugal: precipitation variability associated with large-scale atmospheric circulation. Int. J. Climatol. 18, 619–635.

Dai, A., Fung, I.Y., Del Genia, A.D., 1997. Surface observed global land precipitation variations 1900–88. J. Climate 10, 2943–2962.

Frei, C., Schar, C., 2001. Detection probability of trends in rare events: theory and application to heavy precipitation in the Alpine region. J. Climate 14, 1568–1584.

Gershunov, A., 1998. ENSO influence on intraseasonal extreme rainfall and temperature frequencies in the contiguous United States: implications for long-range predictability. J. Climate 11, 3192–3203.

Gibson, J.K., Kallberg, P., Uppala, A., Hernandes, S., Nomura, A., Serrano, A., 1999. ERA-15 description. Version 2. ECMWF Reanalysis Project Report Series, vol. 1. ECMWF, Reading, England.

Greenwood, J.A., Durand, D., 1960. Aids for fitting the Gamma distribution by maximum likelihood. Technometrics 2, 55–65.

Groismann, P.Y., Karl, T.R., Easterling, D.R., Knight, R.W., Jamason, P.F., Henessy, K.J., Suppiah, R., Page, C.M., Wibig, J., Fortuniak, K., Razuvaev, V.N., Douglas, A., Forland, E., Zhai, P.M., 1999. Changes in the probability of heavy precipitation: important indicators of climatic change. Clim. Change 42, 243–285.

Gulev, S.K., Zolina, O., Grigoriev, S., 2001. Extratropical cyclone variability in the Northern Hemisphere winter from the NCEP/NCAR Reanalysis data. Clim. Dyn. 17, 795–809.

Gulev, S.K., Jung, T., Ruprecht, E., 2002. Interannual and seasonal variability in the intensities of synoptic scale processes in the North Atlantic mid latitudes from the NCEP/NCAR Reanalysis data. J. Climate 15, 809–828.

Hagemann, S., Arpe, K., Bengtsson, L., Kirchner, I., 2002. Validation of precipitation from ERA40 and an ECHAM4.5 simulation nudged with ERA40 data. ERA-40 Project Report Series: 3. Workshop on Reanalysis, 5–9 November 2001. ECMWF, Reading, England, pp. 211–228.

Hayashi, Y., 1982. Confidence intervals of a climatic signal. J. Atmos. Sci. 39, 1895–1905.

Hennessy, K.J., Gregory, J.M., Mitchell, J.F.B., 1997. Changes in daily precipitation under enhanced greenhouse conditions. Clim. Dyn. 13, 667–680.

Hurrell, J.W., 1995. Decadal trends in the North Atlantic Oscillation: regional temperatures and precipitation. Science 269, 676–679.

Hurrell, J.W., van Loon, H., 1997. Decadal variations on climate associated with the North Atlantic Oscillation. Clim. Change 36, 301–326.

Kallberg, P., 2002. An overview of the ERA-40 analyses. ERA-40 Project Report Series. 3. Workshop on Reanalysis, 5–9 November 2001. ECMWF, Reading, England, pp. 31–40.

Kalnay, E., Kanamitsu, M., Kistler, R., Collins, W., Deaven, D., Gandin, L., Iredell, M., Saha, S., White, G., Woollen, J., Zhu, Y., Chelliah, M., Ebisuzaki, W., Higgis, W., Janowiak, J., Mo, K.C., Ropelewski, C., Wang, J., Leetmaa, A., Reynolds, R., Jenne, R., Joseph, D., 1996. The NCEP/NCAR 40-year reanalysis project. Bull. Am. Meteorol. Soc. 77, 437–471.

Kanamitsu, M., et al., 1991. Recent changes implemented into the global forecast system at NMC. Weather. Forecast. 6, 425–435.

Kanamitsu, M., Ebisuzaki, W., Woollen, J., Potter, J., Fiorion, M., 2000. An overview of NCEP/DOE Reanalysis-2. Proc. Conf. 2nd Intl. Conf. On Reanalyses, Reading, England, 23–27 Aug. 1999, WCRP, vol. 109. WMO, Geneva, pp. 1–4. WMO/TD 985.

Kanamitsu, M., Ebisuzaki, W., Woollen, J., Yang, S.-K., Hnilo, J.J., Fiorion, M., Potter, J., 2002. NCEP-DOE AMIP-II Reanalysis (R-2). Bull. Am. Meteorol. Soc. 83, 1631–1643.

Katz, R.W., 1999. Extreme value theory for precipitation: sensitivity analysis for climate change. Adv. Water Resour. 23, 133–139.

Kistler, R., Kalnay, E., Collins, W., Saha, S., White, G., Woollen, J., Chelliah, M., Ebisuzaki, W., Kanamitsu, M., Kousky, V., van den Dool, H., Jenne, R., Fiorino, M., 2001. The NCEP/NCAR 50-year Reanalysis: monthly means CD-ROM and documentation. Bull. Am. Meteorol. Soc. 82, 247–267.

Klein Tank, A.M.G., Koennen, G.P., 2003. Trends in indices of daily temperature and precipitation extremes in Europe, 1946–99. J. Climate 16, 3665–3680.

Klein Tank, A.M.G., et al., 2002. Daily dataset of 20th century surface air temperature and precipitation series for the European Climate Assessment. Int. J. Climatol. 22, 1441–1453.

Maechel, H., Kapala, A., Flohn, H., 1998. Behavior of the centres of action above the Atlantic since 1881. Part I: characteristics of seasonal and interannual variability. Int. J. Climatol. 18, 1–22.

Osborn, T.J., Hulme, M., 1997. Development of a relationship between station and grid-box rain-day frequencies for climate model evaluation. J. Climate 10, 1885–1908.

Pan, H.-L., Wu, W.-S., 1994. Implementing a mass flux convection parameterization package for the NMC medium-range forecast model. Tenth Conf. on Numerical Weather Prediction. Amer. Meteor. Soc., Portland, OR, pp. 96–98.

Plaut, G., Simomnet, E., 2001. Large-scale circulation classification, weather regimes, and local climate over France, the Alps and Western Europe. Clim. Res. 17, 303–324.

Plaut, G., Schuepbach, E., Doctor, M., 2001. Heavy precipitation events over a few Alpine sub-regions and the links with large-scale circulation, 1971–1995. Clim. Res. 17, 285–302.

Semenov, V.A., Bengtsson, L., 2002. Secular trends in daily precipitation characteristics: greenhouse gas simulation with a coupled AOGCM. Clim. Dyn. 19, 123–140.

Stendel, M., Arpe, K., 1997. Evaluation of the Hydrological Cycle in Reanalyses and Observations. Max-Plank-Institut fur Meteorologie, ISSN 0937-1060, report N. 228.

Thom, H.C.S, 1958. A note on the Gamma distribution. Mon. Weather Rev. 86, 117–121.

Tiedtke, M., 1989. A comprehensive mass flux scheme for cumulus parameterization in large-scale models. Mon. Weather Rev. 117, 1779–1800.

Uppala, S., Gibson, J.K., Fiorino, M., Hernandez, A., Kallberg, P., Li, X., Onogi, K., Saarinen, S., 2000. ECMWF second generation reanalysis: ERA40. Proc. Conf. 2nd Intl. Conf. on Reanalyses, Reading, England, 23–27 Aug. 1999, WCRP, vol. 109. WMO, Geneva, pp. 9–13. WMO/TD 985.

von Storch, H., Zwiers, F.W., 1999. Statistical Analysis in Climate Research. Cambridge Univ. Press, Cambridge, 503 pp.

Wanner, H., Broennimann, S., Casty, C., Gyalistras, D., Luterbacher, J., Schmutz, C., Stephenson, D.B., Hoplaki, E., 2001. North Atlantic Oscillation—concept and studies. Surv. Geophys. 22, 282–321.

Watterson, I.G., Dix, M.R., 2003. Simulated changes due to global warming in daily precipitation means and extremes and their interpretation using the Gamma distribution. J. Geophys. Res. 108, 4379.

White, G., 2000. Long-term trends in the NCEP/NCAR Reanalysis. 2nd Int. Conference on Reanalyses, Reading, England, WCRP, vol. 109. WMO, Geneva, pp. 54–57. WMO/TD 985.

Wilks, D.S., 1990. Maximum likelihood estimation for the Gamma distribution using data containing zeros. J. Climate 3, 2285–2298.

Wilks, D.S., 1995. Statistical Methods in Atmospheric Science. Academic Press, London. 467 pp.

Xie, P., Arkin, P.A., 1997. Global precipitation: a 17-year monthly analysis based on gauge observations, satellite estimates, and numerical model outputs. Bull. Am. Meteorol. Soc. 78, 2539–2558.

Yonetani, T., Gordon, H.P., 2001. Simulated changes in the frequency of extremes and regional features of seasonal/annual temperature and precipitation when CO_2 is doubled. J. Climate 14, 1765–1779.

Zolina, O., Kapala, A., Simmer, C., Gulev, S.K., 2004. Estimation of subgrid-scale precipitation component from the daily station data. J. Hydrometeorol. (submitted for publication).

Zwiers, F.W., Kharin, V.V., 1998. Changes in the extremes of the climate simulated by CCC GCM under CO_2 doubling. J. Climate 11, 2200–2222.